

Geochemistry, Geophysics, Geosystems®



RESEARCH ARTICLE

10.1029/2023GC010931

Decadal Monitoring of the Hydrothermal System of Stromboli Volcano, Italy

Cinzia Federico¹ , Salvatore Inguaggiato¹ , Marcello Liotta¹ , Andrea Luca Rizzo^{2,3} , and Fabio Vita¹

¹Istituto Nazionale di Geofisica e Vulcanologia, Sezione di Palermo, Palermo, Italy, ²Istituto Nazionale di Geofisica e Vulcanologia, Sezione di Milano, Milano, Italy, ³Dipartimento di Scienze dell'Ambiente e della Terra, Università di Milano Bicocca, Milano, Italy

Key Points:

- The composition of thermal water and dissolved gases results from the mixing of meteoric marine water and the input of volcanic gases
- Compositional variation is due to the extent of mixing, the solubility-driven fractionation of dissolved gas species
- The gas dissolved in the aquifer has a ³He/⁴He range of 3–4.5 *R_a*, similar to that measured in olivines and pyroxenes

Correspondence to:

S. Inguaggiato,
salvatore.inguaggiato@ingv.it

Citation:

Federico, C., Inguaggiato, S., Liotta, M., Rizzo, A. L., & Vita, F. (2023). Decadal monitoring of the hydrothermal system of Stromboli volcano, Italy. *Geochemistry, Geophysics, Geosystems*, 24, e2023GC010931. <https://doi.org/10.1029/2023GC010931>

Received 2 MAR 2023
Accepted 15 AUG 2023

Author Contributions:

Conceptualization: Cinzia Federico, Salvatore Inguaggiato, Marcello Liotta, Andrea Luca Rizzo, Fabio Vita
Data curation: Salvatore Inguaggiato, Marcello Liotta, Andrea Luca Rizzo, Fabio Vita
Formal analysis: Cinzia Federico, Salvatore Inguaggiato, Marcello Liotta, Andrea Luca Rizzo
Investigation: Cinzia Federico, Salvatore Inguaggiato, Marcello Liotta, Andrea Luca Rizzo, Fabio Vita
Methodology: Salvatore Inguaggiato, Andrea Luca Rizzo, Fabio Vita
Validation: Fabio Vita

Abstract In active volcanoes, magmatic fluids rising toward the surface may interact with shallow waters, thereby forming hydrothermal systems that record variations in magma dynamics at depth. Here, we report on a data set comprising the chemical and isotopic composition of thermal waters and dissolved gases from Stromboli Island (Aeolian Volcanic Arc, Southern Italy) that spans 14 years (2004–2018) of continuous observations. We show that the shallow thermal aquifer of Stromboli results from variable mixing between meteoric water, seawater and magmatic fluids. Gas-water-rock interactions occur, which induce a large spectrum of variation in both water and gas chemistry. These shallow processes do not affect the ³He/⁴He of helium dissolved in thermal waters, which records a magmatic signature that varies in response to changes in magma supply at depth. We show that in periods of more intense volcanic activity, the helium isotopic composition of thermal waters approaches that of the gas emitted from the magma residing at 7–10 km depth. Investigation of hydrothermal waters at active volcanoes is a promising tool to examine magmatic fluids and their shallow circulation, as well as to evaluate the state of activity of a volcano, particularly when summit areas are inaccessible.

1. Introduction

Hydrothermal systems usually form in active volcanoes as a result of the condensation of a saline liquid phase upon decompression of H₂O-rich fluids degassed from magma or by absorption of HCl-rich and SO₂-rich fluids in aquifers fed by meteoric or seawater and the contact of these acidic and hot fluids with the surrounding rocks (Webster & Mandeville, 2007). The shallowest level of hydrothermal systems is often heated by the acidic vapor separated from deeper aquifers. Gas-water-rock interactions occur and trigger a set of chemical-physical processes and reactions that often lead to significant changes in the pristine composition of magmatic fluids. Hydrothermal systems can be found in many volcanoes on Earth, irrespective of the geodynamic setting of formation, as they form in open- or closed-conduit volcanoes, in subaerial or submarine conditions, and consist of one or two phases (liquid and/or vapor) developed into convective fluid cells (Antoine et al., 2009; Caliro et al., 2004, 2007; Chiodini et al., 1995, 2001, 2005; Federico et al., 2010; Finizola et al., 2002; Lupton et al., 2008; Mauri et al., 2018; Osinski et al., 2001; Rizzo et al., 2019; Taran et al., 2017). Hydrothermal systems dissipate much of the energy produced by the volcanic system and may display the first indications of impending crises (e.g., Chiodini et al., 2016). The nature and extent of hydrothermal systems (Finizola et al., 2009; Lénat et al., 2012; Mauri et al., 2018; Revil & Linde, 2006; Revil et al., 2011) influence the occurrence of hazards such as phreatic and phreatomagmatic explosions, and flank collapses (Lorenz & Kurszlauskis, 2007; Weinstein, 2007). The geochemical characterization and monitoring of hydrothermal fluids are of great importance to constrain (a) the composition, temperature, pressure, and redox conditions of the system, (b) the state of activity of the volcano, (c) the evolution of unrest, particularly in those systems where access to high-temperature fumaroles is unsafe (Caliro et al., 2004, 2007; Capasso et al., 1999, 2005; Chiodini et al., 1995, 2001, 2005; Federico et al., 2010; Giggenbach, 1975; S. Inguaggiato & Rizzo, 2004; S. Inguaggiato et al., 2000, 2005, 2010; Lupton et al., 2008; Mauri et al., 2018; Rizzo et al., 2015, 2019; Taran et al., 2017). In many cases, the shallow fluids of meteoric or marine origin feeding the volcanic aquifers may modify the pristine signature of the deep fluids and the signals linked to volcanic activity. Understanding gas–water interaction processes, which modify the pristine physico-chemical characteristics of fluids, sheds light on both the origin of the fluids and the degree of this interaction at depth. In recent years, the study of the volatiles dissolved in the thermal waters of several volcanic systems has provided useful indicators of the origin of these fluids and the processes that modify their chemical and isotope

© 2023 The Authors. *Geochemistry, Geophysics, Geosystems* published by Wiley Periodicals LLC on behalf of American Geophysical Union. This is an open access article under the terms of the [Creative Commons Attribution-NonCommercial License](https://creativecommons.org/licenses/by-nc/4.0/), which permits use, distribution and reproduction in any medium, provided the original work is properly cited and is not used for commercial purposes.

Writing – original draft: Cinzia Federico, Salvatore Inguaggiato, Marcello Liotta, Andrea Luca Rizzo, Fabio Vita
Writing – review & editing: Cinzia Federico, Marcello Liotta, Andrea Luca Rizzo

composition during their ascent toward the surface (Capasso et al., 2005; Federico, Inguaggiato, et al., 2017; S. Inguaggiato et al., 2000, 2005, 2010; Paonita et al., 2016).

Stromboli Island (Aeolian Volcanic Arc, Italy) is an open-conduit volcano characterized by persistent explosive activity, which makes the regular monitoring of fumarole gases in the crater area hazardous (Capasso et al., 2005; Carapezza & Federico, 2000; Rizzo et al., 2009). However, the thermal aquifer identified at the base of the subaerial part of the edifice (Capasso et al., 2005; Carapezza & Federico, 2000; Finizola et al., 2002, 2003, 2009; Revil et al., 2011) represents a safe point of observation to acquire insights into the volcano-hydrothermal system through sampling.

Many geochemical studies on the thermal aquifer, which is accessible via privately drilled wells, have been carried out in the last two decades (Capasso et al., 2005; Carapezza & Federico, 2000; Carapezza et al., 2004; Federico et al., 2008; Grassa et al., 2008; S. Inguaggiato & Rizzo, 2004; Liotta et al., 2006; Madonia et al., 2021; Rizzo et al., 2008, 2009, 2015). These studies revealed (a) the main composition of thermal waters and gases dissolved therein, (b) the influence of shallow marine and meteoric waters (MWs) on the hydrothermal composition, (c) the presence and extent of gas-water-rock interaction processes, and (d) a magmatic signature concerning helium isotopes. These studies brought an invaluable understanding of fluid geochemistry at Stromboli, but most of them took place over short periods, often limited to single effusive eruptions.

In this work, we report on the chemical and isotopic composition of thermal waters and dissolved gases from Stromboli Island over 14 years of observations from 2004 to 2018. We characterize the hydrothermal system of Stromboli, highlighting the main processes occurring therein. The aim is to provide an interpretative framework for the variations in water and gas chemistry, which incorporates the processes of meteoric input, seawater contamination, gas-water-rock exchange, and water mixing, before relating them to volcanological processes. We report on eight thermal water wells located in the area of Stromboli village monitored via 112 sampling campaigns. We show that magmatic fluids re-equilibrate at hydrothermal conditions and the gases collected in the monitored wells show variable relative contents of CO₂, He, and CH₄, the latter being of hydrothermal origin. The variable extent of rock-leaching and seawater/meteoric mixing modulate the chemistry and isotopic ratios of the shallow water. The dissolved gas shows a magmatic signature of ³He/⁴He, comparable to that measured in olivine and pyroxene minerals (Martelli et al., 2014), whose temporal monitoring revealed systematic variations during effusive eruptions and phases of intense volcanic activity.

2. Study Area

2.1. Volcanological Background of Stromboli

Stromboli Island is an active volcano in the Aeolian Archipelago (Italy), which is located in the southeastern Tyrrhenian Sea (Figure 1), and associated with the Quaternary subduction of the African plate below the European plate (e.g., Gasparini et al., 1982). Stromboli was built on a 17-km-thick continental crust (Morelli et al., 1975; Panza et al., 2007) and is characterized by persistent explosive activity from the summit craters (usually every 10–20 min), known throughout the world as “Strombolian activity” (e.g., Rosi et al., 2000). This Strombolian activity is occasionally interrupted by lava effusions and/or violent explosions referred to as “major explosions” and “paroxysms,” which eject large bombs and may occasionally cause hot avalanches, landslides and tsunamis. In the last 35 years, four effusive eruptions occurred in 1985, 2002, 2007, and 2014 (S. Inguaggiato et al., 2018) in addition to many major explosions and lava overflows. Paroxysmal explosions were recorded in 2003, 2007, and two in 2019 (Andronico et al., 2021).

Stromboli erupts magmas belonging to four distinct series, that is, calc-alkaline (CA), high potassium calc-alkaline (HKCA), shoshonitic (SHO), and potassic (KS) (e.g., Francalanci et al., 1988, 1989). All erupted magmas are mafic (SiO₂ <55%, MgO >4%) and exhibit similar subduction-related patterns of trace elements (Francalanci et al., 1993, 2007; Tommasini et al., 2007). The geochemical signature of the primitive batches of the Stromboli magmatic series (CA, HKCA, SHO, KS) is attributed to the partial melting of a mantle wedge, made heterogeneous by the variable metasomatism by fluids released by the subducting slab (Schiavi et al., 2012; Tommasini et al., 2007). Moreover, crustal contamination likely occurred in the KS magmas (Ellam et al., 1989; Francalanci et al., 1993, 2004; Martelli et al., 2014; Schiavi et al., 2012; Tommasini et al., 2007).

The present-day activity of Stromboli belongs to the shoshonitic series and consists of two types of magmas: (a) a high porphyritic (HP) volatile-poor magma, stored at 2–4 km depth below sea level (bsl) that undergoes slow but continuous degassing-induced crystallization and (b) a low porphyritic (LP) volatile-rich magma stored at

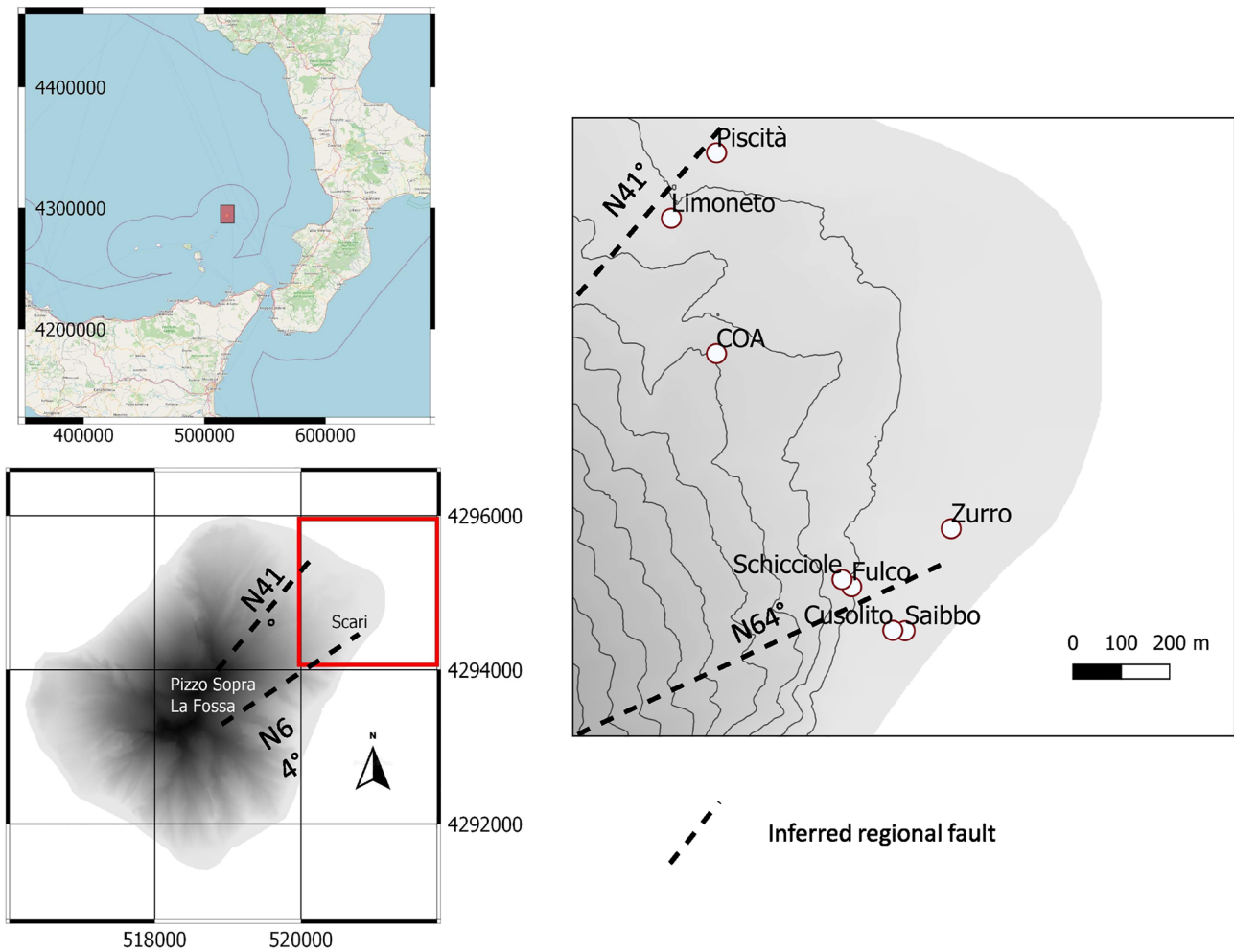


Figure 1. Location of sampling points and main regional faults N41°; N64° (Finizola et al., 2002). The map reference system is ETRS89/UTM 33 N. The red square marks the position of Stromboli Island in Southern Italy.

7–10 km depth bsl, refilled by CO₂-rich magmas rising from the mantle (e.g., Bertagnini et al., 2008; Francalanci et al., 2004; Métrich et al., 2010, 2021). The persistent Strombolian activity of the volcano is maintained in a steady state, driven by the continuous refilling of the shallow magmatic reservoir with deep volatile-rich magmas, together with almost continuous magma emission during ordinary activity (e.g., Landi et al., 2009; Métrich et al., 2010). Magmatic volatiles, which represent the engine of the explosive volcanic activity, are largely emitted from the summit craters during both quiescence and eruptive phases, but they also escape from the soil in the summit area and along the upper flanks of the edifice and at the base of the cone, focused along tectonic lineaments (Carapezza & Federico, 2000; Carapezza et al., 2009; Finizola et al., 2006; S. Inguaggiato et al., 2019, 2020, 2021).

2.2. The Stromboli Thermal Aquifer

2.2.1. Hydrogeology

Previous hydrogeological studies (Madonia et al., 2021; Revil et al., 2011) described the characteristics of the aquifer in this sector of Stromboli. Based on electrical resistivity measurements, soil CO₂ concentrations, temperature, and self-potential measurements, Revil et al. (2011) provided insights regarding the position of shallow aquifers and the extension of the hydrothermal system. They found that self-potential data reveal the position of an unconfined aquifer above the villages of Scari and San Vincenzo. Moreover, they gave evidence of a conductive zone in the central portion of the volcanic edifice, interpreted as the main hydrothermal system, and an advective hydrothermal circulation downward E and NE, in the area of Scari. The boundary between hydrothermal water and groundwater was estimated at about 100 ± 60 m asl, while the intrusion of the seawater

was assumed to be as low as -3 km in depth. More recently, Madonia et al. (2021) indicated that there is a unique groundwater body in the form of a thin lens of fresh water floating above the infiltrating seawater and suggested the existence of a multi-level aquifer, consisting of alternating lavas and pyroclastic deposits.

2.2.2. Chemistry of Groundwater

The thermal waters were studied by Carapezza and Federico (2000), Carapezza et al. (2004), Capasso et al. (2005), and Grassa et al. (2008). The authors found that the chemical composition of thermal waters is the result of mixing in different proportions between seawater and MW, heated by vapor ascending from depth, with limited interaction with the volcanic rocks. They reported temperatures in the range of 35 – 47°C , the water table at depths of 5 – 20 m b.g.l., and a wide range of dissolved salt content ranging from $8,200$ to $40,000$ mg/L, as the result of variable fractions of seawater. The reported average pH values were in the range of 6.31 and 6.97 . The chemical composition of both end-members is modified by the dissolution of a CO_2 -rich gas phase and by leaching the aquifer-hosting rocks. Liotta et al. (2006) also studied the chemical composition of the rainwater which is mainly controlled by the contribution of marine aerosol near the coast, whereas it is strongly influenced by volcanic activity near the summit vents. The hydrogen and oxygen isotopic composition of rainfall shows seasonal variability and correlates with air temperature, while deuterium excess, computed as $d = \delta\text{D}\text{‰} - 8\delta^{18}\text{O}\text{‰}$, has a positive correlation with altitude. Liotta et al. (2006) suggested that the production of volcanic aerosol close to the craters could favor the non-equilibrium condensation of water droplets by diffusional growth of hydrometeors that causes a great deuterium excess as a result of the higher diffusivity of HD^{16}O compared to that of H_2^{18}O . The isotope composition of the meteoric recharge was retrieved from the mean annual volume-weighted values, being between -6.2 and -8.4‰ for $\delta^{18}\text{O}$ and between -35 and -45‰ for δD (vs. the Vienna Standard Mean Ocean Water, V-SMOW) (Liotta et al., 2006).

2.2.3. Chemistry and Carbon Isotopes of Dissolved Gas

The chemical and isotopic composition of dissolved gas in the Stromboli shallow aquifer was discussed by Capasso et al. (2005) and Federico et al. (2008). The air-free composition of the dissolved gas is dominated by CO_2 , with variable amounts of He and CH_4 . While the authors claim a magmatic origin for both CO_2 and He, the CH_4 contents were ascribed to a contribution of fluids from a hydrothermal system.

A wide compositional variability characterizes both the whole aquifer and each sampling site (Capasso et al., 2005; Federico et al., 2008). This variability was ascribed to the heterogeneity of volcanic deposits, made of alternating levels of pyroclastics of different grain sizes, porosity, and permeability, which host small water bodies variably contaminated by seawater and volcanic fluids. The variable enrichment in He and CH_4 compared to an original CO_2 -dominated volcanic gas could be a consequence of modification of the gas during dissolution in the aquifer. Both vapor separation from a hydrothermal aquifer and dissolution in the shallow meteoric aquifer would promote the preferential partitioning of the less-soluble gas species into the vapor phase, namely He and CH_4 compared to CO_2 , and also the isotopic fractionation of gaseous CO_2 compared to dissolved carbon species (Capasso et al., 2005; Federico et al., 2008).

Some of the variability in the sampled fluids was also ascribed to the changeable input of volcanic fluids over time. Carapezza et al. (2004) and Capasso et al. (2005) reported significant variations in the chemical and isotopic composition of CO_2 in all the monitored thermal wells associated with the effusive eruption that occurred in 2002–2003. Values of dissolved CO_2 as high as 75 – 220 cc/L at STP in March–July 2002 were measured 6 months before the onset of the eruption, which was shortly preceded by a one order of magnitude increase in the soil CO_2 flux in the summit area (S. Inguaggiato et al., 2011). Moreover, before the 5 April 2003 paroxysm, Carapezza et al. (2004) and Rizzo et al. (2008) observed a marked decrease in the pH values of 0.1 – 0.5 pH units in the thermal water wells located in the Stromboli village, ascribed to the increased input of CO_2 in the shallow thermal aquifer. S. Inguaggiato, Vita, et al. (2017) and C. Inguaggiato et al. (2017) reported on variations in pCO_2 in two wells for a limited period, related to variations in soil CO_2 fluxes recorded both in Scari (C. Inguaggiato et al., 2017) and at the summit of the volcano in the same period (S. Inguaggiato, Vita, et al., 2017).

2.2.4. Noble Gases

Noble gases are chemically inert, have a low solubility in silicate melts (comparable to that of CO_2) and behave as incompatible elements during mantle melting and magma differentiation (Hilton & Porcelli, 2013). Among noble gases, helium isotopes reported as $^3\text{He}/^4\text{He}$ normalized to the same ratio in atmosphere is the most used tracer due to the different origin of the two isotopes: ^3He is primordial, not renewed and stored in the Earth's interior, ^4He is radiogenic and originates from the radioactive decay of U and Th.

Carapezza and Federico (2000) reported on the noble gas composition (concentration of ^4He and ^{20}Ne , $^4\text{He}/^{20}\text{Ne}$ and $^3\text{He}/^4\text{He}$) of fluids from Stromboli in a fumarole located at Pizzo Sopra La Fossa (Figure 1), called SC5. This fumarole was monitored from 1992 to 1998 and showed $^3\text{He}/^4\text{He}$ values in the range of 2.71–3.55 R_a , indicating a clear magmatic signature. However, the gases showed a variable but significant air contamination, as suggested by $^4\text{He}/^{20}\text{Ne}$ between 1.0 and 3.2, implying an uncertainty in the corrected $^3\text{He}/^4\text{He}$ values. The $^3\text{He}/^4\text{He}$ values measured at SC5 were appreciably lower than those measured at Vulcano Island and Mt Etna, inferring a contribution of radiogenic crustal ^4He to the local fumarolic gas (Carapezza & Federico, 2000).

For the first time in 2002, S. Inguaggiato and Rizzo (2004) studied the noble gas composition of thermal waters from Stromboli within a methodological study aimed at developing and consolidating a technique to determine and monitor the isotope ratio of dissolved He in groundwater. Three wells were selected (Cusolito, Fulco, and Zurro; Figure 1) where water samples were collected. Helium concentrations were in the range $1.4\text{--}6.2 \times 10^{-4}$ cc/L at STP, in the same order of magnitude as that measured by Carapezza and Federico (2000). Neon concentrations ranged between 3.5×10^{-5} and 1.6×10^{-4} cc/l at STP. The $^4\text{He}/^{20}\text{Ne}$ was 3.7–9.6. The $^4\text{He}/^{20}\text{Ne}$ corrected for air contamination (R_c/R_a) was in the range 4.06–4.23 R_a . $^3\text{He}/^4\text{He}$ values of 4.06–4.23 R_a have been found in thermal waters sampled at the base of the subaerial volcanic edifice (S. Inguaggiato & Rizzo, 2004). To explain the lower isotopic signature of SC5, they argued that the water-rock interaction in a hydrothermal system recognized in the summit area by Finizola et al. (2002, 2003) could enhance the contribution of radiogenic ^4He from U and Th decay, thus decreasing the pristine $^3\text{He}/^4\text{He}$ in Pizzo Sopra La Fossa fumaroles. Finally, it has been highlighted that the study of dissolved gases in the thermal waters in Stromboli could be strategic for monitoring purposes, besides validating the technique for the determination of dissolved noble gases (S. Inguaggiato & Rizzo, 2004).

The first data set of noble gas monitoring in thermal waters collected with a roughly monthly frequency between 2002 and 2014 has been reported by Capasso et al. (2005) and Rizzo et al. (2009, 2015). During that period of monitoring, (a) an effusive eruption occurred at Stromboli in 2002–2003 as well as a paroxysmal explosion on 5 April 2003; (b) an effusive eruption occurred in February–April 2007, including a paroxysmal explosion that occurred on 15 March; and (c) an effusive eruption occurred in August–November 2014.

The above-reported studies on time series found that $^3\text{He}/^4\text{He}$ values ranged from 3.4 to 4.5 R_a , with slight or negligible differences among the wells, while the $^4\text{He}/^{20}\text{Ne}$ was in the range of 1–11. These values were comparable to those found by S. Inguaggiato and Rizzo (2004), except for the natural variability related to the persistent activity of Stromboli. In addition, Capasso et al. (2005) showed that the $^3\text{He}/^4\text{He}$ measured in the thermal waters were comparable to the unique value of 4.3 R_a found during the eruption in newly formed fumaroles located close to the north-east crater (Finizola et al., 2002; Finizola & Sortino, 2003). These findings further confirmed that the range of $^3\text{He}/^4\text{He}$ values found in thermal waters is representative of the magmatic signature and can be used for evaluating the state of activity of the volcano. In terms of application to volcano monitoring, the temporal variations of $^3\text{He}/^4\text{He}$ occurred simultaneously in all the thermal water wells (Capasso et al., 2005; Rizzo et al., 2009, 2015). Importantly, the highest $^3\text{He}/^4\text{He}$ values (4.50–4.56 R_a) were always measured during the eruptive phases and were interpreted as due to new input of undegassed LP-like magma and the transfer of its gas toward the surface. After the eruptive phases, relatively high $^3\text{He}/^4\text{He}$ values at all the sampling sites suggested continued fresh input of magma from depth and resumption of Strombolian activity (Capasso et al., 2005; Rizzo et al., 2009, 2015).

The elemental (He, Ne, and Ar) and isotopic (He and Ar) compositions of fluid inclusions hosted in olivine and clinopyroxene from lavas, pyroclastics, and cumulate xenoliths erupted by Stromboli in the last 60 ka contributed in constraining the signature of the magmatic source (Martelli et al., 2014). The authors found that most of the investigated samples exhibit a $^3\text{He}/^4\text{He}$ ratio in the range of 4.0–4.9 R_a , with only the minerals of the KS series showing lower isotopic values ($\leq 3.5 R_a$). This variability was interpreted as being due to a heterogeneous mantle source. In detail, the maximum $^3\text{He}/^4\text{He}$ ratio found in the LP fluid inclusions (i.e., 4.6 R_a) corresponds to the maximum ratio measured in the hydrothermal fluids (Capasso et al., 2005; Rizzo et al., 2009), suggesting that this value can be considered as a marker of the maximum contribution from the LP magma in surface gases.

3. Materials and Methods

3.1. Sampling and In Situ Measurements

Most of the sampling sites are wells located on the northeast side of Stromboli Island (Figure 1), drilled for private use. Limoneto and COA wells were drilled for purely scientific use aimed at groundwater monitoring. We also collected

two samples of dripping water from a cave in the neighborhood of Fulco well (FCDW). The highest piezometric level (0.86 m asl) is measured in the COA well, the farthest from the coast, whereas in the other wells, closer to the coast, a piezometric level of around 0.5 m is measured, with a hydraulic gradient of 1.7 m km^{-1} at COA and 2.0 m km^{-1} at Limoneto. Groundwater monitoring was performed using portable equipment, an electric submersible pump, or on-site plumbing when present. The chemical-physical parameters (pH, temperature, electrical conductivity, and redox potential) were measured in the field using Orion Star A series instruments, equipped with Hamilton electrodes. At the beginning of each sampling activity, the pH-meter was calibrated using at least two buffers. Over the sampling period, the calibration of the pH-meter was verified between one sampling and another by a single-point calibration at pH 7. Calibration of the conductivity meter Orion Star A 122 was performed using the standard of a known concentration that is close to the expected range of conductivity of the water being sampled. The same sampling procedure was used over the entire study period. A submersible pump was placed approximately in the mid-portion of the water column in the wells and switched on for a sufficient duration (15–30 min) to purge the well of the stagnant water, before the sampling. During this stage, pH, electrical conductivity, and turbidity of the water were monitored in order to verify the achievement of adequate purging. Adequate purging is achieved when the pH and electrical conductivity of the water show constant values, and the turbidity has disappeared, resulting in water clarification. The condition of stability requires pH variations within 0.1 unit and conductivity variations within about 5%.

For the determination of dissolved major ions, water samples were filtered with $0.45 \mu\text{m}$ filters and stored in LD-PE (low-density polyethylene) bottles. The aliquots to be analyzed for cation content were also acidified to $\text{pH} \approx 2$ with Suprapur(R) HNO_3 . The alkalinity was determined by titration with HCl (0.1 N) on an untreated aliquot.

Water samples, used for dissolved gas and isotope determinations, were collected in serum bottles and sealed underwater with Teflon-faced rubber septa and aluminum seals, to minimize atmospheric contamination. Glass bottles were filled while avoiding turbulent water flow by keeping the pump flow rate low. In addition, silicon tubes were inserted directly down to the bottom of the serum bottle while it is immersed in a basin filled with the same water to be sampled (Liotta & Martelli, 2012). The bottles were sealed by crimping the Teflon-faced rubber septum using an aluminum seal.

3.2. Chemical and Isotopic Analyses

Major elements were analyzed in the laboratory of INGV-Palermo using ion chromatography systems (Dionex-Thermo ICS 1100) in suppressed mode, equipped with a column AS14A and a precolumn (AG14A) for anions (F^- , Cl^- , Br^- , and SO_4^{2-}), and a column CS12A and precolumn CG12A for cations (Li^+ , Na^+ , K^+ , Mg^{++} , and Ca^{++}). The columns work under a continuous flow of a carbonate–bicarbonate eluent for anions and a methanesulfonic acid eluent for cations. The precision and accuracy of the method are described in Prano and Liotta (2018) and are usually below 5%. During each analytical session, a certified material was analyzed to check the accuracy.

Dissolved gases were sampled and analyzed according to the method described by Capasso and Inguaggiato (1998), which is based on the equilibrium partitioning of gas species between a liquid and a gas phase after the introduction of a host gas (Ar) into the sample. The analysis was performed in the INGV-Palermo laboratories using a gas chromatograph (Perkin Elmer Clarus 500) equipped with a double detector (a thermal conductivity detector (TCD) and a flame ionization detector (FID) with a methanizer) and Ar as the carrier gas. H_2 , O_2 , N_2 , and CO_2 were measured using the TCD detector, while CH_4 and CO were determined using the FID detector coupled to the methanizer (Capasso & Inguaggiato, 1998). Standard mixtures were routinely analyzed before any analytical session, and the analytical precision was always better than 5%. An automated procedure was used to determine the $\delta^{13}\text{C}$ of total dissolved inorganic C in water ($\delta^{13}\text{C}_{\text{TDIC}}$) (Capasso et al., 2005). C-isotope ratios ($^{13}\text{C}/^{12}\text{C}$) were measured using a mass spectrometer (Delta V Plus) connected online to the GasBench II system. The results were reported in ‰ versus the V-PDB standard, with a precision better than $\pm 0.1\%$.

The analysis of He and Ne concentrations, $^3\text{He}/^4\text{He}$, and $^4\text{He}/^{20}\text{Ne}$ of the gases dissolved in thermal waters was performed in the laboratories of INGV-Palermo (Vita et al., 2023). Noble gases were extracted from the water following an optimized method developed by S. Inguaggiato and Rizzo (2004) and based on that proposed by Capasso and Inguaggiato (1998) for the study of gases dissolved in water. Two aliquots of water samples were sampled. After introducing the extracted gases in a system of ultra-high-vacuum purification lines, ^3He , ^4He , and ^{20}Ne and the $^4\text{He}/^{20}\text{Ne}$ ratios were determined by separately admitting He and Ne into a split flight tube mass spectrometer (GVI-Helix SFT, for He analysis) and a multi-collector mass spectrometer (Thermo-Helix MC plus, for Ne analysis). He and Ne purification and separation were carried out based on standard purification

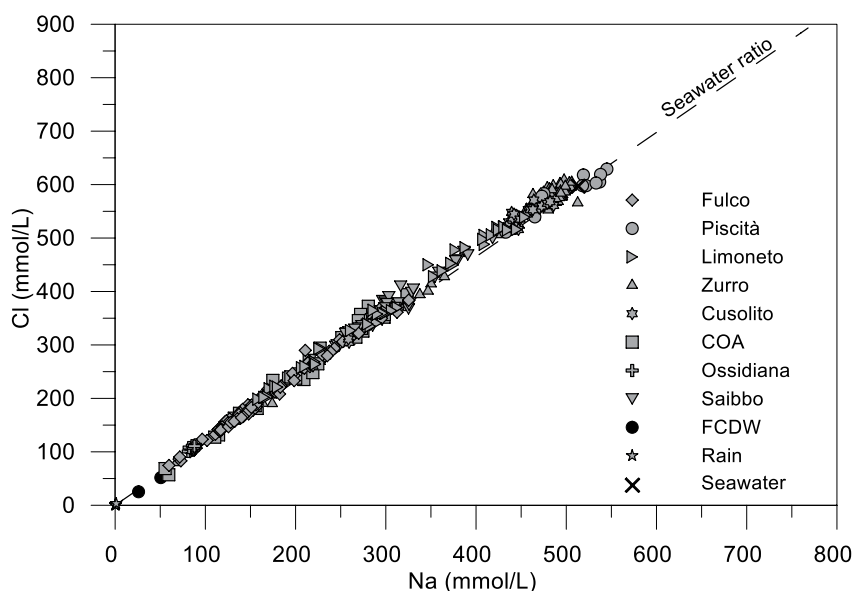


Figure 2. Well data plotted on a chlorine (Cl)—sodium (Na) diagram. The mean amount-weighted composition of rainwater (Liotta et al., 2006) and dripping water from a cave in the neighborhood of Fulco well are also plotted.

procedures (Rizzo et al., 2015, 2016). The $^3\text{He}/^4\text{He}$ ratio is expressed as R/R_a (R_a being the He isotope ratio of air and equal to 1.39×10^{-6}), and the analytical error is generally below 0.7%. The $^3\text{He}/^4\text{He}$ values were corrected for the atmospheric contamination based on the measured $^4\text{He}/^{20}\text{Ne}$ ratio, as follows:

$$R_c/R_a = \left[R_M/R_a \left(\frac{4\text{He}}{20\text{Ne}} \right)_M - \left(\frac{4\text{He}}{20\text{Ne}} \right)_A \right] / \left[\left(\frac{4\text{He}}{20\text{Ne}} \right)_M - \left(\frac{4\text{He}}{20\text{Ne}} \right)_A \right] \quad (1)$$

where subscripts M and A refer to measured and air-saturated water (ASW) theoretical values, respectively [$(4\text{He}/20\text{Ne})_A = 0.285$]. The corrected $^3\text{He}/^4\text{He}$ ratios reported in the text are expressed as R_c/R_a values.

4. Results

4.1. Chemistry of Groundwater

The whole data set covers the period 2004–2018 and includes data relating to the wells Fulco, Cusolito, Zurro, Limoneto, Ossidiana, Saibbo, COA, and Piscità. All the data produced in this work are publicly available in the Earthchem data repository (Vita et al., 2023). We also report and discuss the geochemical data relative to two samples of dripping water from a cave in the neighborhood of Fulco well (FCDW, Fulco Cave Dripping Water) that we consider representative of the infiltrating water in that area. The water temperature is almost constant over time at each site (as previously observed by Grassa et al. (2008)); mean values are 35.8°C at Zurro, 41.5°C at Fulco, 40.1°C at Saibbo, 40.1°C at Limoneto, 41.9°C at COA, 42.8°C at Cusolito, 34.8°C at Ossidiana, and 32.7°C at Piscità. The pH values range between 5.72 and 7.43 and are systematically lower at COA, Saibbo, and Fulco sites, with average values of 6.33, 6.33, and 6.39, respectively. All the other sites exhibit higher average pH values: 6.70 at Cusolito, 6.75 at Limoneto, 6.93 at Ossidiana, 6.86 at Zurro, and 7.11 at Piscità. All the samples fall around the line representative of the Na/Cl ratio in seawater, between the FCDW sample and the Mediterranean seawater composition (Figure 2) (Capasso et al., 2005; Carapezza & Federico, 2000; Carapezza et al., 2004; Grassa et al., 2008). When taking into account the isotope composition of thermal waters, all the samples fall between the meteoric end-member and seawater (Figure 3).

4.2. Chemistry and Carbon Isotope Composition of the Dissolved Gas

We present the dissolved gas composition and carbon isotope composition of dissolved carbon (Vita et al., 2023). The dissolved gas is dominated by CO_2 in all wells, with contents ranging from 1.5 to 290 cc/L at STP. Nitrogen contents range from 3 to 23 cc/L at STP, whereas dissolved O_2 was always below the concentration of ASW (7 cc/L at STP) with N_2/O_2 ratios much higher than in ASW at STP ($\text{N}_2/\text{O}_2 \sim 2$). The CH_4 contents range from 1×10^{-4} to 5×10^{-2} cc/L at STP.

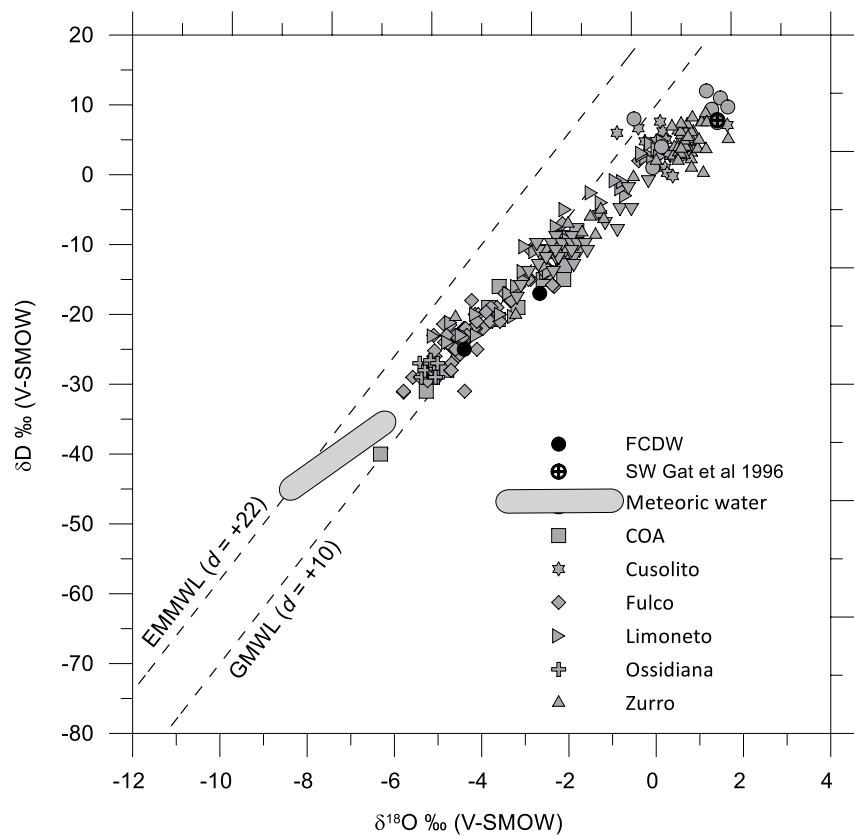


Figure 3. Diagram showing δD versus $\delta^{18}O$ in the groundwater of Stromboli. The gray area defines the composition of the meteoric recharge (Liotta et al., 2006). The dashed lines are the Global Meteoric Water Line and the Eastern Mediterranean Meteoric Water Line (Gat & Carmi, 1970). Dripping water at Fulco cave (FCDW) is also plotted as well as the Mediterranean seawater (SW) (Gat et al., 1996).

The triangular diagram of Figure 4 shows a wide variation in the relative proportions of He, CO₂, and CH₄ in the dissolved gas phase, in both the whole aquifer and each sampled well. In particular, Fulco and Ossidiana wells are characterized, on average, by the highest relative amounts of CO₂, although some samples from both wells are richer in CH₄. The wells COA, Cusolito, and Zurro show a stronger enrichment in both He and CH₄, with few samples richer in CH₄. Limoneto and Piscità wells are characterized by the most evident enrichment in He.

The Stromboli thermal aquifer is characterized by a wide range of CO₂ contents, observed even in wells located in a restricted area and, in some cases, in a given well over time. The high CO₂ contents in the aquifer are matched by correspondingly more positive values of the isotope composition of the dissolved CO₂ ($\delta^{13}C_{CO_2}$, Vita et al., 2023), computed from the measured $\delta^{13}C_{TDC}$ (Vita et al., 2023). The pristine isotope composition of gaseous CO₂ is retrieved from the measured $\delta^{13}C_{TDC}$ by applying the fractionation factor between total dissolved carbon (TDC) and gaseous CO₂ ($\alpha_{TDC-CO_2,g}$), computed according to the weighted contribution of the enrichment factors ϵ between CO₂ and each dissolved carbon species, as described by Capasso et al. (2005) and Federico et al. (2008). As observed in Figure 5, the highest dissolved CO₂ contents, measured in Fulco well, are associated with values of $\delta^{13}C_{CO_2}$ of about -1.5% . The lowest CO₂ contents, characterized by relatively more negative $\delta^{13}C_{CO_2}$ values, were measured in the wells Piscità and Zurro.

4.3. Chemistry of Noble Gases

Here, we integrate the existing data on He and Ne concentrations, $^4He/^{20}Ne$ and $^3He/^4He$ with new data that cover part of the inter-eruptive periods between 2004 and 2018 (Vita et al., 2023). Helium concentrations are in the range of 9.2×10^{-5} – 2.3×10^{-3} cc/L at STP (Figure 6), with the highest values measured in COA, Limoneto, and Piscità wells and the lowest in the Fulco well. Neon concentrations range between 4.2×10^{-5} and 2.4×10^{-4} cc/l at STP. The $^4He/^{20}Ne$ varies between 0.9 and 17.3 (Figures 6 and 7). In general, the R_f/R_a values do not show

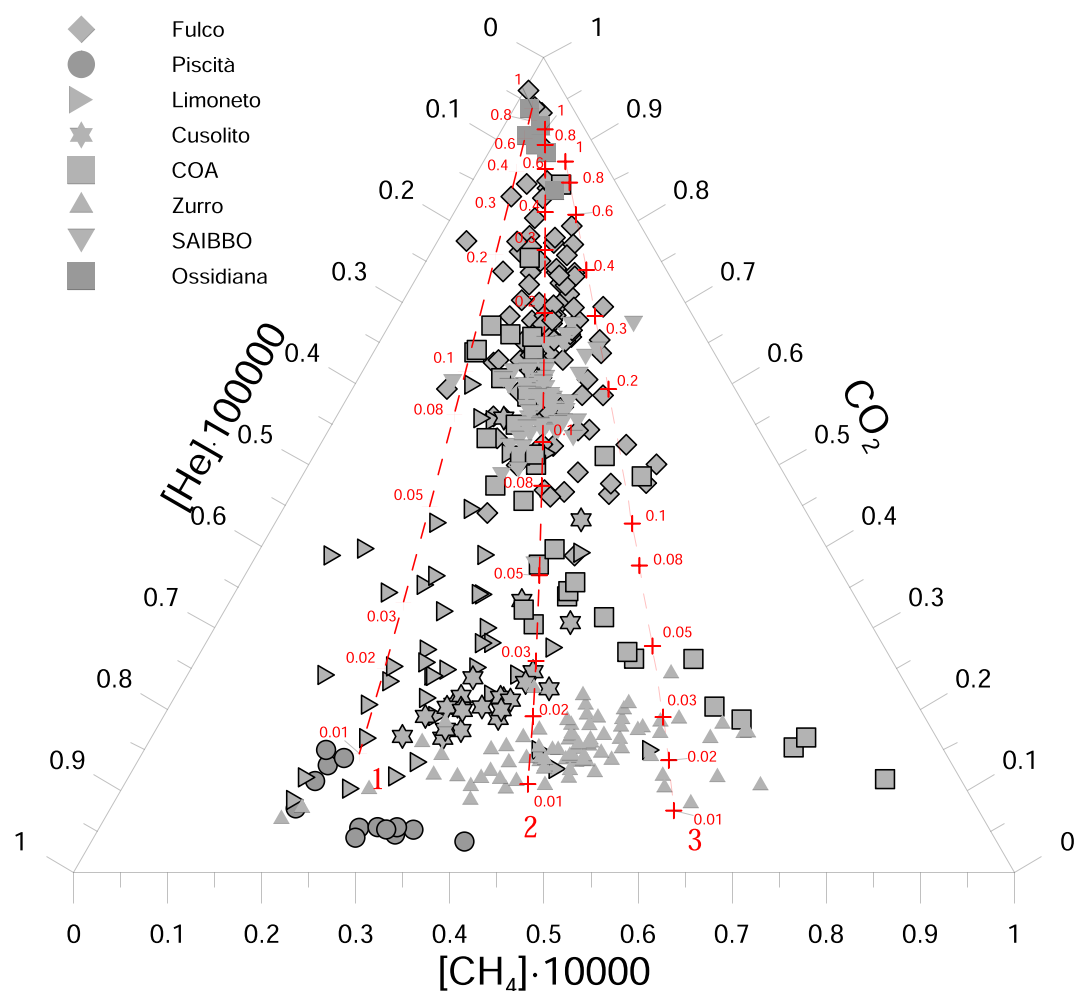


Figure 4. Relative contents of He, CH₄, and CO₂ (cc/L at STP). Curves 1, 2, and 3 represent the modeled composition of the dissolved gas, obtained by partial dissolution, in a shallow aquifer at 40°C, of a gas having initial CH₄/CO₂ ratios of 5×10^{-5} , 1×10^{-4} , and 2×10^{-4} respectively, and He/CO₂ = 2.4×10^{-5} , hypothesized to be separated from an underlying boiling aquifer. The crosses on the red curves refer to different fractions of residual gas after dissolution (F_2 in Equation A1, see Appendix A).

significant differences among the wells (Figure 7). The $^3\text{He}/^4\text{He}$ corrected for air contamination (R/R_a) is in the range of 3.89–4.53 R_a (Figure 8). These ranges are in the same order of magnitude as those measured by Carapezza and Federico (2000), S. Inguaggiato and Rizzo (2004), Capasso et al. (2005), and Rizzo et al. (2009, 2015).

5. Discussion

5.1. Processes Controlling Water Chemistry

Each site sampled shows chemical variability due to different degrees of mixing between meteoric recharge and seawater. Fresh groundwater usually lies upon brackish waters, and fluctuations of the water table can occur in coastal sites as an effect of tides (Singaraja et al., 2018) and the seasonal variability of the meteoric recharge (Liotta et al., 2006). As a consequence, even if the sampling of thermal water is always carried out using the same protocol (pumping flux, depth of the pump, duration of pumping before collecting samples, etc.), samples from the same sites show temporal variability in their salinity, the extent of which varies depending on the site features.

Among the elements that are enriched by the interaction with aquifer-hosting rocks (Capasso et al., 2005), K has the higher mobility since it does not precipitate as secondary phases, unlike Ca and Mg (e.g., calcite, Mg-calcite and gypsum), recognized in the hydrothermal alteration of the surface rocks (Finizola et al., 2002). Due to these characteristics, the element K offers the opportunity to evaluate the extent of water-rock interaction. In Figure 9,

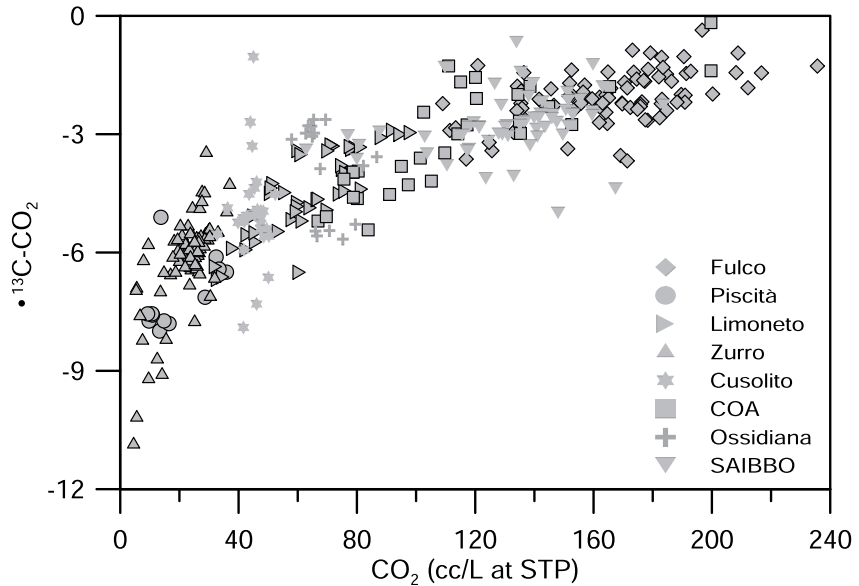


Figure 5. $\delta^{13}\text{C}_{\text{CO}_2}$ versus dissolved CO_2 . Values of $\delta^{13}\text{C}_{\text{CO}_2}$ are computed from measured $\delta^{13}\text{C}_{\text{TDC}}$ (method given in the text).

K is plotted versus Cl. All the samples exhibit a clear enrichment in K with respect to seawater. Samples from Fulco, Cusolito, Limoneto, Ossidiana, and Saibbo wells (with few exceptions probably due to direct seawater intrusion) fall on a line between Cusolito and FCDW. The alignment is indicative of a mixing process between a saline end-member (among the samples of Cusolito, EM3 in Figure 9) and the infiltrating water (FCDW and the poor saline samples from well Fulco, EM1 in Figure 9), being both enriched in K. This implies that shallow fresh waters interact with the host-rocks and leach K. Conversely, samples from the Zurro well result from mixing between a saline end-member with high Cl content (one sample from Piscità well, EM2 in Figure 9) and a shallow end-member (represented by poor saline samples from well COA, EM4 in Figure 9). Samples from the COA well result from mixing between a saline end-member (EM3) enriched in K and a shallow end-member (EM4 in Figure 9). For both Zurro and COA samples, the shallow end-member (EM4) does not show a clear K-enrichment and probably reflects the rainfall composition, suggesting fast infiltration of MW and limited interaction with the hosting rocks.

The dissolution and hydration of magmatic CO_2 promotes the chemical weathering of rocks. If equilibrium is attained in the measured pH range, the carbonic acid dissociates as HCO_3^- . Total alkalinity is a measure of CO_2 -water interaction and provides information about the paths through which CO_2 reaches the aquifer. In Figure 10 we show that samples from Fulco, Cusolito, Limoneto, Ossidiana, and Saibbo define a negative relationship between Cl concentration and total alkalinity. Since freshwater floats on saline water, such a correlation

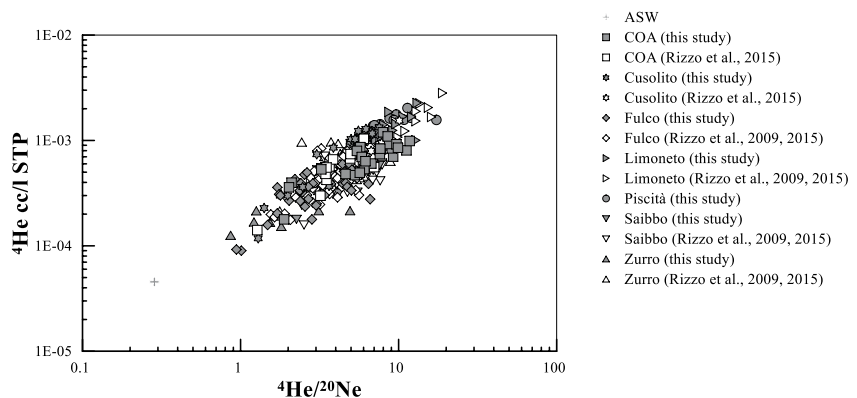


Figure 6. $^4\text{He}/^{20}\text{Ne}$ versus ^4He cc/L at STP in the thermal wells of Stromboli. Air-saturated water with $^4\text{He}/^{20}\text{Ne} = 0.285$ and $^4\text{He} = 4.55 \times 10^{-5}$ cc/L at STP is plotted for comparison.

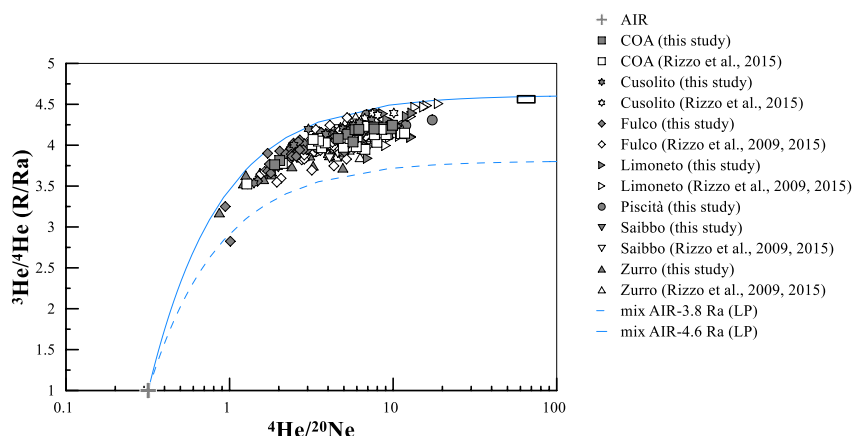


Figure 7. $^4\text{He}/^{20}\text{Ne}$ versus $^3\text{He}/^4\text{He}$ expressed as R/R_a . The two curves indicate mixing lines between an atmospheric component with $^4\text{He}/^{20}\text{Ne} = 0.318$ and $R/R_a = 1$ and two possible magmatic end members with $^4\text{He}/^{20}\text{Ne} = 100$, as observed in other analogous investigations (e.g., Lages et al., 2021; Rizzo et al., 2015, 2022; Robidoux et al., 2020), and 3.8–4.6 R_a that includes all the data variability observed in 2004–2018. The rectangle reports the maximum range of values measured in fluid inclusions from low porphyritic magma minerals (Martelli et al., 2014).

implies that most of the CO_2 dissolved in water does not come from depth but is carried by infiltrating waters. The large flux ($5,000\text{--}40,000 \text{ g m}^{-2} \text{ d}^{-1}$) of CO_2 degassing from soils (S. Inguaggiato et al., 2019 and reference therein) as well as the identification of a low-resistivity body in the summit area of the volcano (Revil et al., 2011 and references therein), are consistent with the idea that meteoric waters infiltrating the summit area interact with CO_2 rising through fractures, favoring water-rock interaction and an increase of the total alkalinity. A fraction of the TDC reaches the basal aquifer as dissolved CO_2 . At the Zurro site, the freshwater end-member exhibits low total alkalinity, indicating limited interaction between meteoric waters and CO_2 . Consequently, we observe a negative relationship between Cl and total alkalinity (Figure 10). At the COA site, samples display a large dispersion of compositions since the well is the most elevated (70 m asl) and deepest. As a consequence, the well intercepts several lithological layers and receives different types of infiltrating waters with different CO_2 contents.

The meteoric origin of fresh groundwater (highlighted by Grassa et al. (2008) using water stable isotopes) is demonstrated in Figure 3. All the samples fall between the isotope composition of the Mediterranean seawater and the local meteoric end-member defined by Liotta et al. (2006).

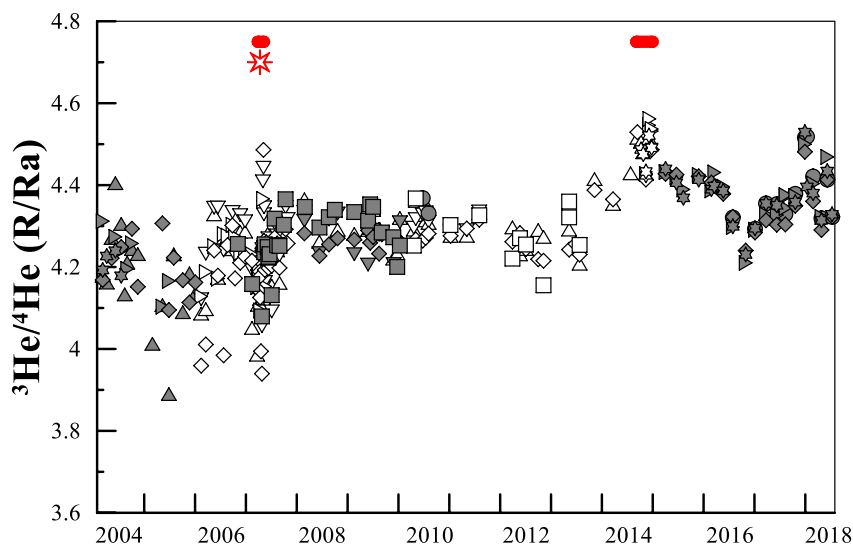


Figure 8. Time series of R/R_a values measured in gases dissolved in the thermal waters of Stromboli. Red bars indicate the periods of lava effusion, the red symbol the paroxysmal explosion occurred on the 15 March 2007.

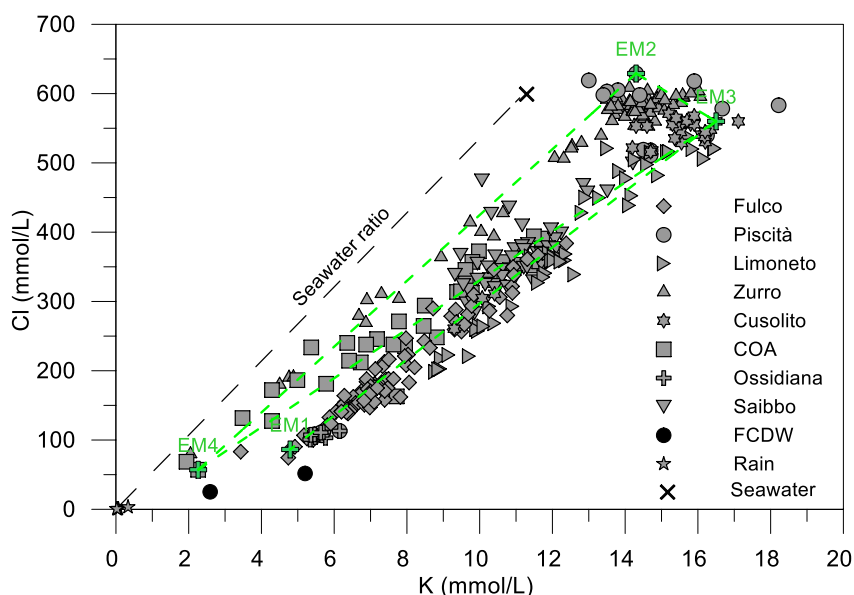


Figure 9. Stromboli groundwater samples displayed on a plot of Cl against K. All the samples show enrichment in K compared to the seawater ratio. The mean amount-weighted composition of rainwater (Liotta et al., 2006) and dripping water (FCDW) from a cave in the neighborhood of Fulco well are also plotted.

5.2. Gas/Water Interaction Processes: Dissolution-Related Gas Fractionation

The relative proportions of CO_2 , CH_4 , and He vary in the different sites and, in the same site, over time (Figures 4 and 5); moreover, the samples with the highest CO_2 contents also have a $\delta^{13}\text{C}$ isotope signature close to -1.5‰ , which is in the range of values measured in the SC5 and Fossa fumaroles, in the summit area (Capasso et al., 2005; Carapezza & Federico, 2000; Finizola et al., 2003; Rizzo et al., 2009), as well as in fluid inclusions of olivine and clinopyroxene crystals separated from the San Bartolo ultramafic cumulates (Gennaro et al., 2017). The CO_2 -poorer samples, namely Limoneto, Piscità, and Cusolito, have lower $\delta^{13}\text{C}$ values and are enriched in both He and CH_4 by more than two orders of magnitude compared to ASW. Although the relationship shown in Figure 5, observed in other volcanic and non-volcanic aquifers (Chiodini et al., 2000; Federico et al., 2002; Ohsawa

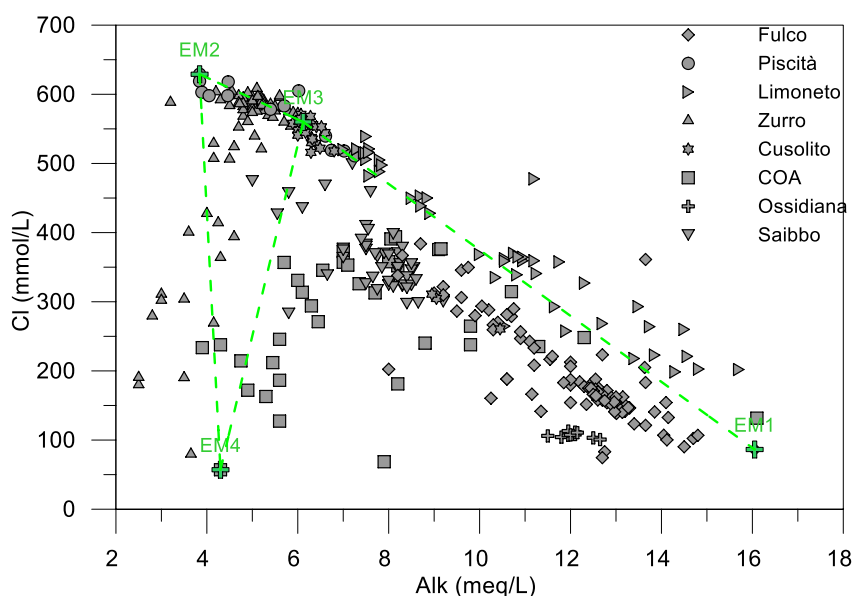


Figure 10. Stromboli groundwater samples displayed on a plot of Cl against total alkalinity. With the exception of Zurro and COA, samples exhibit a negative relationship between Cl and total alkalinity (see text for details).

et al., 2002; Yamada et al., 2011), has generally been interpreted as resulting from mixing between volcanic CO₂-rich gases and soil CO₂-poor gases with more negative carbon isotope composition (typical of organic carbon) other studies have interpreted negative δ¹³C values as due to the fractionation of CO₂ during multistep dissolution of CO₂ in water (Simmons & Christenson, 1994 and references therein). The data set presented here suggests that some portions of the aquifer are flushed by a He-CH₄-rich gas phase, derived from a volcanic gas modified during interaction with a multilevel hydrothermal aquifer, where the gases could separate and dissolve from one level to another (Capasso et al., 2005; Federico et al., 2008). The multilevel aquifer is probably hosted by the alternating levels of lavas and pyroclastics in the subsoil of the Scari area, as suggested by Madonia et al. (2021). During gas-water interaction, different gas species fractionate according to their solubility in water, described in Appendix A.

The extent of the Rayleigh fractionation described above depends on the solubility of gases and the fraction of remaining gas (F) (Equation A1 in Appendix A), which could be considered as a proxy for the relative masses of the CO₂-rich gas and the water with which it interacts. The larger the amount of gas interacting with a given volume of water in an interval of time, the smaller the relative amount of gas removed upon dissolution, and the fraction of residual gas F (Equation A1 in Appendix A) would be slightly lower than 1. In this case, the dissolved gas composition would not be significantly different from the initial composition and would represent the deep volcano-hydrothermal gas. The samples richest in CO₂ from the Fulco well correspond to the highest values of F in Figure 4, which indicates that this well taps water levels entered by volcanic gases that are little modified by gas-water exchange. The area of Scari is considerably affected by the input of volcanic CO₂ (S. Inguaggiato et al., 2013; S. Inguaggiato, Diliberto, et al., 2017) and some wells in this area, namely Fulco and Saibbo, have the highest dissolved CO₂ contents (290 and 180 cc/L at STP, respectively). On the contrary, in areas where the amount of gas interacting with the groundwater is lower, the extent of fractionation is larger, the fraction F of residual gas is significantly lower than 1, and the residual gas composition is predicted to be significantly different from the initial gas composition. In the Stromboli aquifer, this modified gas composition characterizes the most saline samples, with Cl contents as high as about 550 mmol/L, namely those collected in the Piscità well and some samples from the Limoneto well. Due to the significant contribution of seawater, these wells are characterized by relatively higher pH values (from 6.7 to 7.1), and this plays a significant role in the fractionation process due to the ability of basic aquifers to trap CO₂.

In Figure 11, the groundwater He/CO₂ ratios are plotted versus the Cl contents, chosen as a proxy for seawater contribution. The selected wells, namely COA, Limoneto, and Piscità, display variable Cl contents and, as discussed in Section 5.1, result from variable mixing between saline and meteoric-derived end members (between the end-members EM1 and EM2 and EM4 and EM3). The highest He/CO₂ values, measured in the most saline well (Piscità), have the lowest CO₂ and alkalinity contents (Figure 10) and the highest He contents, which implies a mechanism of helium enrichment in the saline aquifer in response to the lower solubility in water of He compared to CO₂ (e.g., Capasso et al., 2005; Sander, 2015 and references therein). As observed in Figure 4, these samples show the highest He/CO₂ ratios and correspond to values of the fraction F of residual gas lower than 0.01. This well taps water levels where the input of volcanic gases is probably minor and/or the effect of CO₂ trapping in the aquifer at depth is locally enhanced by higher contamination of seawater.

5.3. Variations of Water Chemistry and Dissolved Gases

The He/CO₂ and CH₄/CO₂ ratios measured in water samples are shown, together with the theoretical curves derived from the processes of gas dissolution and mixing, in Figure 12. As in Figure 4, the theoretical curves are plotted by assuming three different initial CH₄/CO₂ values, from 5 × 10⁻⁵ to 2 × 10⁻⁴, and a He/CO₂ ratio of 2 × 10⁻⁵. Gas dissolution is likely a cause of the variable gas concentrations in the aquifer. Moreover, as evidenced by water chemistry, mixing between end member waters of different salinities, and different gas contents, can add further variability in the different wells and in a single well over time. Salinity and gas contents are sometimes related, as shown in Figure 11, which makes the processes of fractionation and mixing seldom distinguishable.

We hypothesize various mixing trends which could account for the variability observed among the wells and in a single well over time (Figures 12 and 13). The composition of air-saturated MW and air-saturated seawater (SW) are plotted for comparison. The CO₂ contents of samples decrease as Cl contents increase (Figure 13a), whereas CH₄ and He increase with Cl contents. Neither the air-saturated MW nor the air-saturated seawater (SW) contribute significantly to the studied samples, which implies that a volcano-hydrothermal gas phase, variably enriched in CO₂, CH₄, or He, prevails over atmospheric gases, although the samples are meteoric or marine in origin. Samples from the Zurro and Cusolito wells display a fairly narrow range of Cl contents (except for some

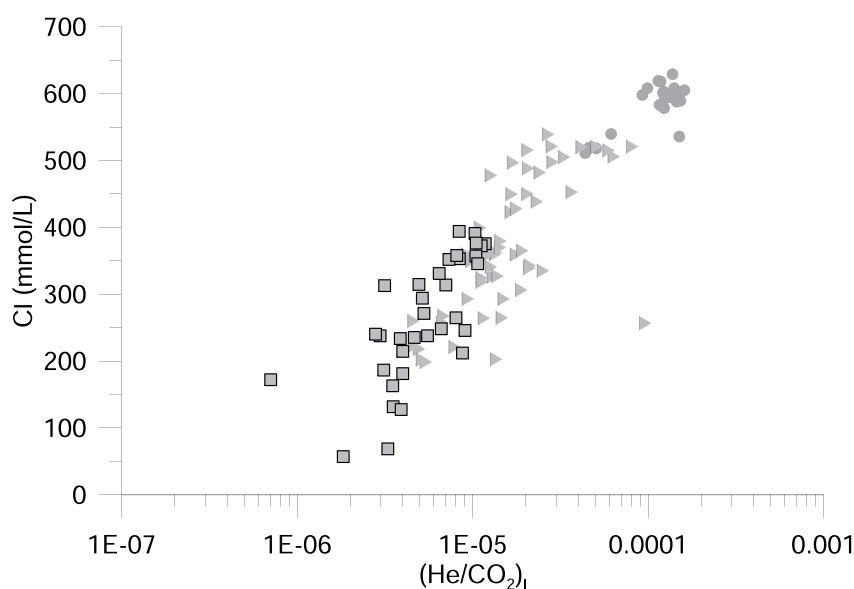


Figure 11. Chlorine versus dissolved He/CO₂ ratios in the wells COA, Limoneto, and Piscità. Symbols as in Figure 2.

samples mixed with purely MW), despite slightly variable CO₂, CH₄ and He contents. These two wells, both in the Scari area, are characterized by rather high He/CO₂ values (Figure 12). The salinity of the samples from these wells is fairly homogeneous over time, so we might assume that the mixing of different water types is negligible. In this case, the changes in gas composition would be due to the variable contribution of gas enriched in He upon dissolution and gas less fractionated and richer in CH₄ and CO₂.

Mixing between end members of different salinities, and different CO₂, He, and CH₄ contents is demonstrated for wells Limoneto, COA, SAIBBO, and Fulco, as evident in the graphs of Figure 13, and could be the origin of the variable composition detected in these wells. End member EM1 is meteoric in origin, rich in CO₂, and relatively poor in CH₄ and He; the gas has a CH₄/CO₂ ratio of around 2.5×10^{-5} and a He/CO₂ ratio of 2.4×10^{-5} , and is the less fractionated by dissolution in the shallow aquifer (curve 2 in Figure 12). End member EM4, meteoric in origin like EM1, has a CH₄-He-rich and CO₂ poorer composition, probably deriving from the fractionation after dissolution (curve 2 in Figure 12); EM3, prevalently of marine origin, lies on the same Rayleigh curve as EM4, at higher He and lower CO₂ contents, due to further fractionation. The mixing of EM1 and EM4 end members (representing the poorest saline samples from Fulco and COA) with EM3, already noted in Figure 9 to explain the composition of samples from COA, is confirmed by the gas composition. The composition of some samples of COA may be explained by a further contribution of CH₄, as evident in Figure 13b. The processes of fractionation upon dissolution and mixing are clearly closely related, and only when the water composition is constant would it be possible to isolate and examine the variations exclusively related to fractionation. The temporal variations, at least in some cases (e.g., Limoneto well, Figure 14), are probably more affected by the mixing between water bodies of different salinities and gas composition. In other cases, the effects of mixing or fractionation upon dissolution are not clearly distinguishable and the scatter in the data compared to the theoretical mixing curves confirms the occurrence of both processes.

The mixing between water bodies of different compositions is not surprising in a stratified aquifer, in a coastal area, where seawater-contaminated water levels lie below MW levels and extend inland for tens or hundreds of meters. Additionally, the contribution of the magmatic-hydrothermal gas is uneven in the shallow aquifer and likely variable over time, thus increasing the spatial and temporal variability. In a single well, the dominance of one type of water or another can result from the variable meteoric input over time, from variations of the seawater level (Capasso et al., 2014), or modification of water circulation due to variations of crustal strain, as an effect of volcanic activity (Federico, Longo, et al., 2017 and references therein).

5.4. Chemistry of Noble Gases

As already highlighted and modeled in Section 5.2, the concentration (in cc/L at STP) of ⁴He dissolved in thermal waters from different wells differs mostly in response to its preferential partitioning into the vapor phase

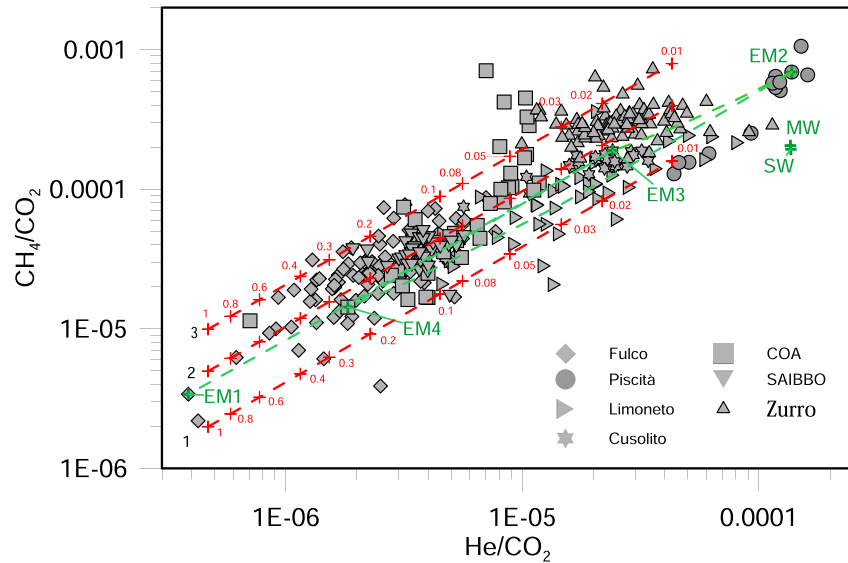


Figure 12. Scatter plot of CH_4/CO_2 versus He/CO_2 ratios measured in well waters. Gas concentrations are expressed as cc/L at STP. Curves 1, 2, and 3 represent the modeled composition of the dissolved gas, obtained by partial dissolution, in a shallow aquifer at 40°C , of a gas having initial CH_4/CO_2 ratios of 5×10^{-5} , 1×10^{-4} , and 2×10^{-4} respectively, and $\text{He}/\text{CO}_2 = 2.4 \times 10^{-5}$, hypothesized to be separated from an underlying boiling aquifer. The crosses on the red curves refer to different fractions of residual gas after dissolution (F2 in Equation A1, Appendix A). Colored lines represent the mixing between different end members (green crosses), marine or meteoric in origin, characterized by different gas compositions. The composition of air-saturated water (MW) and seawater (SW) at 15°C is plotted for comparison (ASW: $\text{CO}_2 = 0.38$ cc/L, $\text{He} = 4.5 \times 10^{-5}$ cc/L, $\text{CH}_4 = 7.8 \times 10^{-5}$ cc/L at STP; ASSW: $\text{CO}_2 = 0.32$ cc/L, $\text{He} = 3.8 \times 10^{-5}$ cc/L, $\text{CH}_4 = 5.9 \times 10^{-5}$ cc/L at STP; Liotta & Martelli, 2012).

compared to CO_2 . Instead, ^{20}Ne concentrations do not show the same variability among the wells, although ^{20}Ne and ^4He solubility in water is comparable (Sander, 2015). In detail, the concentration of ^{20}Ne varies over a range of values that includes the theoretical value in ASW and is comparable among the different wells, irrespective of the extent of the fractionation due to gas-water interaction. This indicates that the mixing between magmatic and atmospheric fluids modulates the variability in ^{20}Ne concentration, further supporting the idea that hydrothermal vapor mixes with the shallower meteoric aquifer, variably contaminated by seawater (Capasso et al., 2005; Grassa et al., 2008 and this work). Consequently, atmospheric Ne entirely masks that of magmatic origin, which we expect to have a concentration of 2–3 orders of magnitude lower. We therefore argue that ^{20}Ne cannot be used to evaluate the extent of gas-water interaction in the different wells and, more importantly, that the variability of $^4\text{He}/^{20}\text{Ne}$ is mostly modulated by the variability in ^4He concentrations, as can be visualized in Figure 6. The Limoneto and Piscit  wells, which show the highest enrichment in ^4He , also display the highest $^4\text{He}/^{20}\text{Ne}$ values (Figure 6), which could impact the correction of atmospheric contamination, which is based on the $^4\text{He}/^{20}\text{Ne}$ ratios. Nevertheless, considering that $^4\text{He}/^{20}\text{Ne}$ values are generally at least one order of magnitude higher than in ASW ($^4\text{He}/^{20}\text{Ne} = 0.285$), even in those wells less modified by the fractionation due to gas-water interaction, we point out that the R_c/R_a corrected values generally differ from measured R/R_a values of less than $0.2 R_a$, leading us to consider the correction we applied reliable. Some exceptions to this are a few samples from the Cusolito, Fulco, and Zurro wells sampled during 2004–2008 that showed among the lowest ^4He content and $^4\text{He}/^{20}\text{Ne}$ next to or below 1, which probably led to an uncertainty in the correction of $^3\text{He}/^4\text{He}$ and an underestimation of R/R_a values.

5.4.1. Statistical Evaluation of $^3\text{He}/^4\text{He}$ Ratios in the Thermal Aquifer

The regular monitoring of $^3\text{He}/^4\text{He}$ at Stromboli allows a statistical evaluation of the data set. Because $^3\text{He}/^4\text{He}$ ratios are not fractionated by gas-water interaction in the hydrothermal aquifer, they preserve their original signature and are thus used within the INGV-Palermo monitoring protocol. We already noted that there is no difference in the $^3\text{He}/^4\text{He}$ signature among the various wells, therefore our discussion concerns the whole data set. Considering the discrete sampling of the seven thermal wells, a total of 511 measurements of $^3\text{He}/^4\text{He}$ were carried out during 2004–2018. The He isotopic ratios vary between 3.74 and 4.56 R_a with a mean \pm standard deviation of

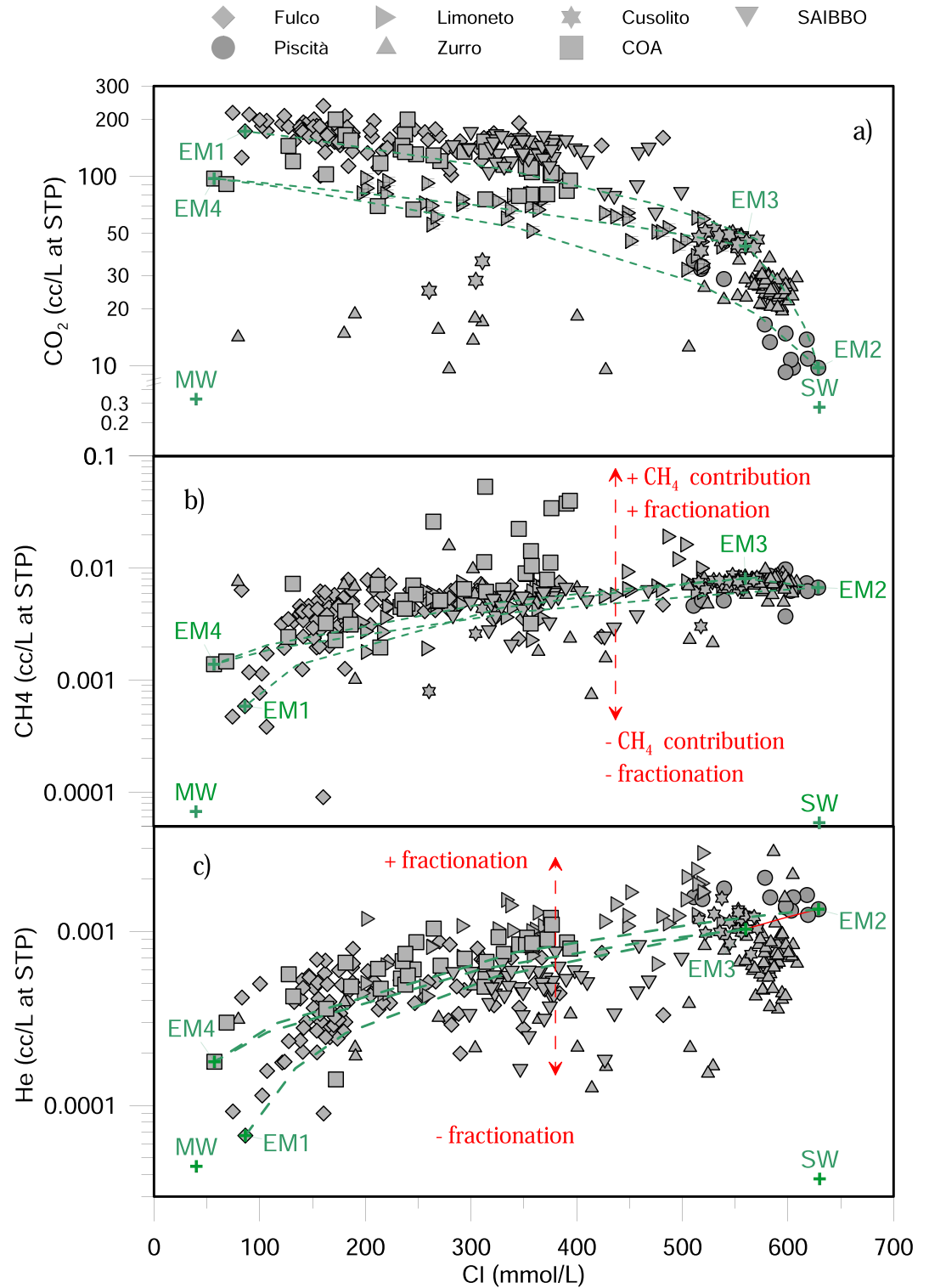


Figure 13. (a) Scatter plot of Cl versus CO₂ contents measured in well waters. Colored lines represent the mixing between different end members, marine or meteoric in origin, characterized by different CO₂ contents. The composition of air-saturated water (MW) and seawater (SW) is plotted for comparison; (b) scatter plot of Cl versus CH₄ contents measured in well waters. Green lines represent the mixing between different end-members, marine or meteoric in origin, characterized by different CH₄ contents; (c) scatter plot of Cl versus He contents measured in well waters. Green lines represent the mixing between different end members, marine or meteoric in origin, characterized by different He contents.

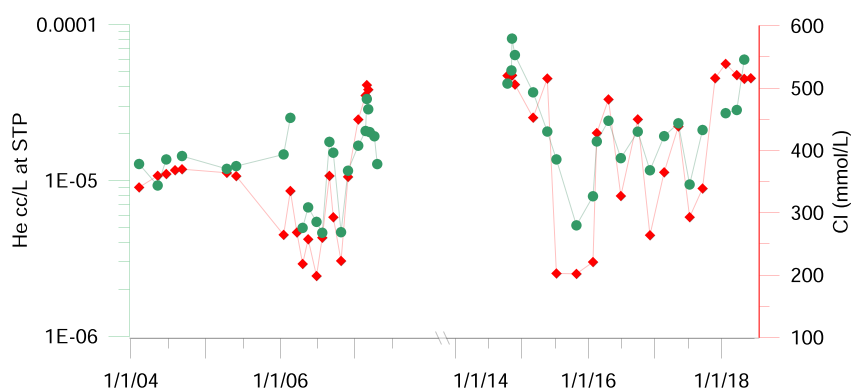


Figure 14. Time trends of He (left axis) and Cl (right axis) in well Limoneto.

$4.24 \pm 0.13 R_a$. In terms of frequency, 63 measurements fall below $4.1 R_a$, equivalent to 12% of the data set, 398 between 4.1 and $4.4 R_a$, equivalent to 78%, and 50 above $4.4 R_a$, equivalent to 10% (Figure 15). Considering that (a) magma replenishments by poorly degassed melts are characterized by increasing $^3\text{He}/^4\text{He}$ values (Capasso et al., 2005; Martelli et al., 2014; Rizzo et al., 2009, 2015), (b) the maximum values measured in phenocrysts of LP magma are about $4.6 R_a$ (Martelli et al., 2014), and (c) the highest $^3\text{He}/^4\text{He}$ values (4.50 – $4.56 R_a$) were always measured during eruptive phases characterized by weeks to months of lava effusion (Martelli et al., 2014; Rizzo et al., 2009, 2015), we conclude that $^3\text{He}/^4\text{He}$ values exceeding $4.4 R_a$ represent phases of dominant degassing of the LP magma, able to potentially feed high magmatic activity.

5.4.2. Variations of $^3\text{He}/^4\text{He}$ Ratios in Relation to Volcanic Activity

To the best of our knowledge, this is the first time that a data set of 14 years of regular measurements of $^3\text{He}/^4\text{He}$ is presented and discussed in a single volcanic system, offering a unique opportunity to better comprehend the short- and long-term evolution of the magmatic activity of Stromboli. The sampled wells have a comparable range of R_c/R_a values (3.7 – $4.5 R_a$) and temporal variations of $^3\text{He}/^4\text{He}$ that occurred almost simultaneously (Figure 8) (Capasso et al., 2005; Rizzo et al., 2008, 2009, 2015). This is confirmed for the periods of monitoring 2004–2005, 2008–2009, and 2015–2018 that are presented in this study for the first time, supporting the idea that the magmatic fluids dissolving in the hydrothermal aquifer have a common source. However, an important difference in R_c/R_a values can be observed between 2002–2007 and 2008–2018: during 2002–2007, the range of $^3\text{He}/^4\text{He}$ varied between 3.7 and $4.5 R_a$ with a mean \pm standard deviation of $4.19 \pm 0.13 R_a$, whereas during 2008–2018 it moves from 4.2 to $4.6 R_a$ with a mean of $4.34 \pm 0.08 R_a$ (Figure 8). The entire period of monitoring (2002–2018) has a mean $^3\text{He}/^4\text{He}$ of $4.24 \pm 0.13 R_a$. In detail, since 2008 onward we have not measured $^3\text{He}/^4\text{He}$ lower than $4.2 R_a$ (except one sample from COA), in contrast to what was observed from 2001 to 2007, and there is a reduced variability in the $^3\text{He}/^4\text{He}$ ratios of each well (Figure 8). However, the highest R_c/R_a values never exceeded $4.6 R_a$ during 2002–2018. We suggest that the differences between the two periods could be due to a modification of the degassing path and the magmatic activity of the volcano (Calvari et al., 2014), which could have favored an enhanced contribution of the ^3He -rich LP melt.

During 2004–2014, R_c/R_a values ≥ 4.4 were measured during and/or in the proximity of the effusive eruptions of 2007, and 2014, and in periods of an increased occurrence of major explosions (Bevilacqua et al., 2020), as in 2017–2018. These values approached the maximum $^3\text{He}/^4\text{He}$ (i.e., $4.6 R_a$) measured by Martelli et al. (2014) in fluid inclusions hosted in olivine and clinopyroxene from LP volatile-rich pumices. Therefore, the temporal variations of the $^3\text{He}/^4\text{He}$ ratio can be explained as a mixing of volatiles persistently emitted from LP magma ($^3\text{He}/^4\text{He}$ ratio $\geq 4.6 R_a$) located in the deep (>7 – 10 km) portions of the plumbing system, with those degassed from batches of magma resident in the shallow portions of the plumbing system up to the HP reservoir (~ 2 km below the sea level; e.g., Métrich et al., 2010, 2021 and references therein). This model was already proposed to explain the variability in the composition of plume gases emitted from the craters (Aiuppa et al., 2010). In addition, we recall that the continuous refilling of the shallow magma body by deep volatile-rich magmas, together with the continuous magma emission, controls the steady state of the Stromboli plumbing system (e.g., Landi et al., 2009; Métrich et al., 2010). The shallow batches of magma would reasonably have a $^3\text{He}/^4\text{He}$ signature (not yet constrained) lower than LP magma. This signature would result from the addition of radiogenic ^4He , produced from U and Th contained in differentiated rocks in contact with the magma, to the residual helium dissolved at

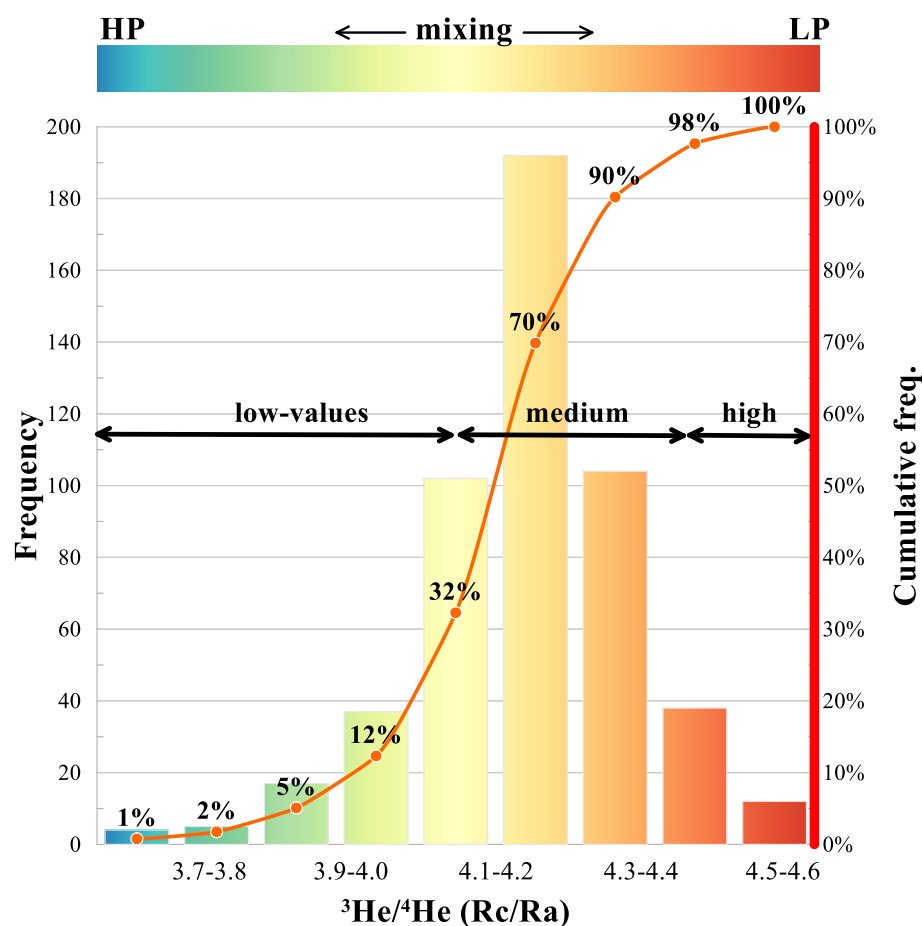


Figure 15. Frequency and cumulative frequency distribution of $^3\text{He}/^4\text{He}$ in Stromboli thermal wells, based on 511 measurements carried out between 2004 and 2018. Considering the analysis of the frequency of occurrence of R_c/R_a values over 14 years of monitoring and taking into account the maximum value measured in fluid inclusions of low porphyritic (LP) minerals (Martelli et al., 2014), the variability of R_c/R_a values is reported as a function of variable extents of mixing between fluids degassed from an LP magma, having ratios as high as $4.6 R_a$, and those from an high porphyritic magma, supposed to have the lowest R_c/R_a values recorded in the time series.

low concentrations in the extensively degassed melts. We cannot exclude that part of this shallow contamination occurs within the hydrothermal system. The temporal variations as well as the absolute values of $^3\text{He}/^4\text{He}$ measured in the fluids resulting from the hypothesized mixing and last dissolving in the hydrothermal aquifer of Stromboli, would largely be regulated by the mass rate of volatiles degassed from the LP magma, which depends on the magma dynamics at depth. Further studies aimed at better constraining the $^3\text{He}/^4\text{He}$ signature of magmas residing in the shallowest portions of the plumbing system and feeding ordinary activity of Stromboli (i.e., HP magma), as well as the path and depth of helium degassing from the mantle, would enable quantitative refinement of this interpretative model.

From November 2014 until April 2016, the R_c/R_a values remained high ($\sim 4.4 R_a$) while the resumption of Strombolian activity was ongoing. After April 2016, the $^3\text{He}/^4\text{He}$ decreased to average values, similar to almost 80% of the data set (Figure 8). Since September 2017, an increase of $^3\text{He}/^4\text{He}$ ratios was observed with values as high as $4.5 R_a$ at the end of November 2017 (Figure 8). After this peak, R_c/R_a values varied around medium-to-medium-high values until June 2018. We highlight that during 2017–2018, the activity at Stromboli was characterized by an increase in the rate of occurrence of Strombolian explosions as well as by the occurrence of several explosions of major intensity and lava overflows (Giudicepietro et al., 2019). During the same period, S. Inguaggiato et al. (2019) reported a progressive increase of CO_2 degassing from the soil in the summit area, further supporting the idea that the level of activity of Stromboli was increasing again in that period.

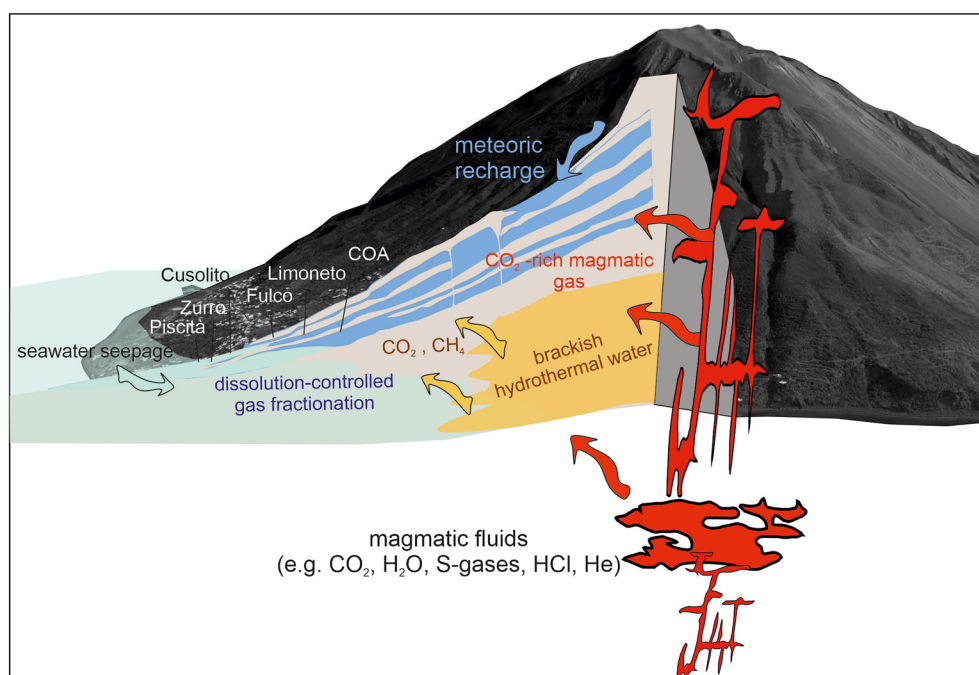


Figure 16. Interpretative model of the shallow thermal aquifer obtained by merging the outcomes of Finizola et al. (2010), Revil et al. (2011), Madonia et al. (2021), and the elaborations of the present work.

6. Interpretative Model and Conclusive Remarks

The long-term monitoring of the Stromboli basal aquifer has allowed the development of a comprehensive framework of the interactions among magmatic-hydrothermal fluids and shallow water. The complexity related to the presence of MW, extensively contaminated by seawater and modified by water-rock exchanges, the reactivity of many of the volcanic gas species, and their different solubility in water, requires some caution when interpreting the observed variations in both water and gas chemistry. The monitored wells tap an unconfined meteoric aquifer variably contaminated by seawater and CH_4 -rich hydrothermal fluids (Figure 16) and are characterized by different CO_2 and He contents. As observed in the Piscit  well, the CO_2 -poor and CH_4 -He-rich composition, together with a temperature higher than 30°C , would be compatible with the interaction with hot volcanic fluids, whose composition is modified by the removal of CO_2 in deeper and, probably, saline water levels, promoted by a relatively low gas flux, according to a mechanism of Rayleigh's fractionation, as described in Section 6.2. The contribution of CH_4 observed in all the monitored wells is probably derived from the boiling of a typical hydrothermal system. In some cases, (either in seawater-derived samples such as Zurro and Cusolito or meteoric-derived samples, such as COA and Limoneto), the hydrothermal gas undergoes further fractionation during its traveling toward the shallower levels of the aquifer.

The compositional variability of the groundwater leads to difficulty in ascertaining the variable contribution over time of the gas of different origins (hydrothermal or prevalently magmatic), possibly modified by dissolution. Probably, variations in gas composition not paralleled by variations in water composition could be ascribed to a variable input of magmatic or hydrothermal gases, to variation in their composition, and/or to Rayleigh's type fractionation, whereas variations in water chemistry point to the mixing between waters, different in both chemistry and gas contents. Rainfall, fluctuations of the seawater level and the water table head in the wells should be routinely monitored to determine the hydrological causes of the variations in water chemistry. The long-term monitoring of helium isotopes in thermal waters has demonstrated that (a) thermal waters have dissolved helium with a magmatic signature that varies in response to medium-to long-term changes in magmatic dynamics at depth and represents a safe method for monitoring the activity of the volcano; (b) low to ordinary activity is generally characterized by $^3\text{He}/^4\text{He}$ values below 4.4 Ra, whereas $^3\text{He}/^4\text{He}$ values greater than 4.4 Ra probably derive from a higher contribution of gas emitted from the LP magma, which may prelude an increase in the eruptive activity.

Appendix A

A1. Chemical Fractionation of Gas as an Effect of Dissolution

The chemical fractionation upon dissolution can be reliably modeled by a Rayleigh's type process, according to the equation (Albarède, 1995; Capasso et al., 2005):

$$\left(\frac{[G_1]}{[G_2]}\right)_{\text{liq}} = \frac{K_{H,2}}{K_{H,1}} \cdot \left(\frac{[G_1]}{[G_2]}\right)_{\text{gas},i} \cdot F_2^{\left(\frac{K_{H,2}}{K_{H,1}} - 1\right)} \quad (\text{A1})$$

where G_1 and G_2 are two gas species, the subscripts liq and gas, i refer to the liquid and the initial gas phase, respectively; F_2 is the residual fraction of the gas species 2, KH is Henry's constants of the two gas species.

In the following, we compute the evolution of He/CO₂ and CH₄/CO₂ ratios according to Equation A1, by assuming He and CH₄ as species 1, and CO₂ as species 2, respectively. In Figure 4, the theoretical composition of the dissolved gas, after the removal of an increasing amount of gas upon dissolution in water, is plotted. The initial gas compositions (i.e., $([G_1]/[G_2])_{\text{gas},i}$) in Equation A1 are selected to best fit the observed data. The different curves refer to three different initial CH₄/CO₂ ratios.

The Henry's constants were computed at 40°C, and their values are 144,000 and 50,560 bar mol mol⁻¹, for He and CH₄, respectively. The KH computed for CO₂ (2263 bar mol mol⁻¹ at 40°C) is reduced by the effect of CO₂ hydration, which also depends on pH and on the dissociation of carbonic acid (see Capasso et al., 2005). The used value is 1,440 bar mol mol⁻¹, computed at pH = 6 and 40°C.

As explained by Capasso et al. (2005), the retrieved initial He/CO₂ ratios (2×10^{-5}) are higher than those measured on average in a fumarole sampled in the Pizzo area (SC5; Capasso et al., 2005) and measured in fluid inclusions (Gennaro et al., 2017) (He/CO₂ ratio ranging from 3×10^{-6} to 10^{-5}), and this implies a probable enrichment in He during the vapor separation from an underlying biphasic aquifer, and particularly for a small fraction of separated gas. The modeled initial CH₄/CO₂ contents span from 5×10^{-5} to 2×10^{-4} and are higher than those measured in the SC5 fumarole (Capasso et al., 2005; Carapezza & Federico, 2000), suggesting a variable CH₄ production in different portions of the hydrothermal aquifer or different periods, besides an additional enrichment after vapor separation.

Madonia et al. (2021) suggested the existence of a stratified (multilevel) hydrothermal aquifer, with temperatures that could be progressively higher, in the deeper and inner parts of the island. The hypothesized fractionation upon dissolution in the shallow aquifer would produce a progressive enrichment in He and CH₄ and depletion of CO₂, toward a gas composition, which in the studied aquifer is characterized by He contents as high as 2.5×10^{-3} cc/L at STP and CO₂ contents as low as 10 cc/L at STP.

Data Availability Statement

All the data produced in this work are publicly available in the Earthchem data repository (Vita et al., 2023).

Acknowledgments

The authors wish to thank their colleagues at the Istituto Nazionale di Geofisica e Vulcanologia of Palermo for their contribution in collecting samples and analyzing data. All the chemical and isotopic data were produced in the Geochemical Laboratories of INGV Palermo. The three anonymous Reviewers and the Editor Marie Edmonds are acknowledged for their comments, which greatly helped to improve the manuscript. This research was funded by the INGV-DPCN (Italian National Institute of Geophysics and Volcanology-Italian National Department for Civil Protection) volcanic surveillance program of Stromboli volcano. ObFu 0304.010.

References

- Aiuppa, A., Bertagnini, A., Métrich, N., Moretti, R., Di Muro, A., Liuzzo, M., & Tamburello, G. (2010). A model of degassing for Stromboli volcano. *Earth and Planetary Science Letters*, 295(1–2), 95–204. <https://doi.org/10.1016/j.epsl.2010.03.040>
- Albarède, F. (1995). *Introduction to geochemical modeling*. Cambridge University Press.
- Andronico, D., Del Bello, E., D'Oriano, C., Landi, P., Pardini, F., Scarlato, P., et al. (2021). Uncovering the eruptive patterns of the 2019 double paroxysm eruption crisis of Stromboli volcano. *Nature Communications*, 12(1), 4213. <https://doi.org/10.1038/s41467-021-24420-1>
- Antoine, R., Baratoux, D., Rabinowicz, M., Fontaine, F., Bachelery, P., Staudacher, T., et al. (2009). Thermal infrared image analysis of a quiescent cone on Piton de la Fournaise volcano: Evidence of convective air flow within an unconsolidated soil. *Journal of Volcanology and Geothermal Research*, 183(3–4), 228–244. <https://doi.org/10.1016/j.jvolgeores.2008.12.003>
- Bertagnini, A., Métrich, N., Francalanci, L., Landi, P., Tommasini, S., & Conticelli, S. (2008). Volcanology and magma geochemistry of the present-day activity: Constraints on the feeding system. In S. Calvari, S. Inguaggiato, G. Puglisi, M. Ripepe, & M. Rosi (Eds.), *Learning from Stromboli*, *Geophysical Monograph* (Vol. 182, pp. 19–38). American Geophysical Union.
- Bevilacqua, A., Bertagnini, A., Pompilio, M., Landi, P., Del Carlo, P., Di Roberto, A., et al. (2020). Major explosions and paroxysms at Stromboli (Italy): A new historical catalog and temporal models of occurrence with uncertainty quantification. *Scientific Reports*, 10(1), 17357. <https://doi.org/10.1038/s41598-020-74301-8>
- Caliro, S., Caracausi, A., Chiodini, G., Ditta, M., Italiano, F., Longo, M., et al. (2004). Evidence of a recent input of magmatic gases into the quiescent volcanic edifice of Panarea, Aeolian Islands, Italy. *Geophysical Research Letters*, 31(7), L07619. <https://doi.org/10.1029/2003gl019359>

- Caliro, S., Chiodini, G., Moretti, R., Avino, R., Granieri, D., Russo, M., & Fiebig, J. (2007). The origin of the fumaroles of La Solfatara (Campi Flegrei, South Italy). *Geochimica et Cosmochimica Acta*, 71(12), 3040–3055. <https://doi.org/10.1016/j.gca.2007.04.007>
- Calvari, S., Bonaccorso, A., Madonia, P., Neri, M., Liuzzo, M., Salerno, G. G., et al. (2014). Major eruptive style changes induced by structural modifications of a shallow conduit system: The 2007–2012 Stromboli case. *Bulletin of Volcanology*, 76(7), 841. <https://doi.org/10.1007/s00445-014-0841-7>
- Capasso, G., Carapezza, M. L., Federico, C., Inguaggiato, S., & Rizzo, A. (2005). Geochemical monitoring of the 2002–2003 eruption at Stromboli volcano (Italy): Precursory changes in the carbon and helium isotopic composition of fumarole gases and thermal waters. *Bulletin of Volcanology*, 68(2), 118–134. <https://doi.org/10.1007/s00445-005-0427-5>
- Capasso, G., Favara, R., Francofonte, S., & Inguaggiato, S. (1999). Chemical and isotopic variations in fumarolic discharge and thermal waters at Vulcano Island (Aeolian Islands, Italy) during 1996: Evidence of resumed volcanic activity. *Journal of Volcanology and Geothermal Research*, 88(3), 167–175. [https://doi.org/10.1016/s0377-0273\(98\)00111-5](https://doi.org/10.1016/s0377-0273(98)00111-5)
- Capasso, G., Federico, C., Madonia, P., & Paonita, A. (2014). Response of the shallow aquifer of the volcano-hydrothermal system during the recent crises at Vulcano Island (Aeolian Archipelago, Italy). *Volcanological and Geothermal Records*, 273, 70–80. <https://doi.org/10.1016/j.jvolgeores.2014.01.005>
- Capasso, G., & Inguaggiato, S. (1998). A simple method for the determination of dissolved gases in natural waters: An application to thermal waters from Vulcano Island. *Applied Geochemistry*, 13(5), 631–642. [https://doi.org/10.1016/s0883-2927\(97\)00109-1](https://doi.org/10.1016/s0883-2927(97)00109-1)
- Carapezza, M. L., & Federico, C. (2000). The contribution of fluid geochemistry to the volcano monitoring of Stromboli. *Journal of Volcanology and Geothermal Research*, 95(1–4), 227–245. [https://doi.org/10.1016/s0377-0273\(99\)00128-6](https://doi.org/10.1016/s0377-0273(99)00128-6)
- Carapezza, M. L., Inguaggiato, S., Brusca, L., & Longo, M. (2004). Geochemical precursors of the activity of an open-conduit volcano: The Stromboli 2002–2003 eruptive events. *Geophysical Research Letters*, 31(7), L07620. <https://doi.org/10.1029/2004gl019614>
- Carapezza, M. L., Ricci, T., Ranaldi, M., & Tarchini, L. (2009). Active degassing structures of Stromboli and variations in diffuse CO₂ output related to the volcanic activity. *Journal of Volcanology and Geothermal Research*, 182(3–4), 231–245. <https://doi.org/10.1016/j.jvolgeores.2008.08.006>
- Chiodini, G., Cioni, R., Marini, L., & Panichi, C. (1995). Origin of the fumarolic fluids of Vulcano Island, Italy, and implications for volcanic surveillance. *Bulletin of Volcanology*, 57(2), 99–110. <https://doi.org/10.1007/bf00301400>
- Chiodini, G., Frondini, F., Cardellini, C., Parello, F., & Peruzzi, L. (2000). Rate of diffuse carbon dioxide Earth degassing estimated from carbon balance of regional aquifers: The case of central Apennine, Italy. *Journal of Geophysical Research*, 105(B4), 8423–8434. <https://doi.org/10.1029/1999jb900355>
- Chiodini, G., Granieri, D., Avino, R., Caliro, S., Costa, A., & Werner, C. (2005). Carbon dioxide diffuse degassing and estimation of heat release from volcanic and hydrothermal systems. *Journal of Geophysical Research*, 110(B8), B08204. <https://doi.org/10.1029/2004JB003542>
- Chiodini, G., Marini, L., & Russo, M. (2001). Geochemical evidence for the existence of high temperature brines at Vesuvio volcano, Italy. *Geochimica et Cosmochimica Acta*, 65(13), 2129–2147. [https://doi.org/10.1016/s0016-7037\(01\)00583-x](https://doi.org/10.1016/s0016-7037(01)00583-x)
- Chiodini, G., Paonita, A., Aiuppa, A., Costa, A., Caliro, S., De Martino, P., et al. (2016). Magmas near the critical degassing pressure drive volcanic unrest towards a critical state. *Nature Communications*, 7(1), 13712. <https://doi.org/10.1038/ncomms13712>
- Ellam, R. M., Hawkesworth, C. J., Menzies, M. A., & Rogers, N. W. (1989). The volcanism of southern Italy: Role of subduction and relationship between potassic and sodic alkaline magmatism. *Journal of Geophysical Research*, 94(B4), 4589–4601. <https://doi.org/10.1029/jb094ib04p04589>
- Federico, C., Aiuppa, A., Allard, P., Bellomo, S., Jean-Baptiste, P., Parello, F., & Valenza, M. (2002). Magma-derived gas influx and water-rock interactions in the volcanic aquifer of Mt. Vesuvius, Italy. *Geochimica et Cosmochimica Acta*, 66(6), 963–981. [https://doi.org/10.1016/s0016-7037\(01\)00813-4](https://doi.org/10.1016/s0016-7037(01)00813-4)
- Federico, C., Brusca, L., Carapezza, M. L., Cigolini, C., Inguaggiato, S., Rizzo, A., & Rouwet, D. (2008). Geochemical prediction of the 2002–2003 Stromboli eruption from variations in CO₂ and Rn emissions and in helium and carbon isotopes. In *Learning from Stromboli and its 2002–2003 eruptive crisis*, American Geophysical Union Geophysical Monograph Series (Vol. 182, pp. 117–128). AGU.
- Federico, C., Capasso, G., Paonita, A., & Favara, R. (2010). Effects of steam-heating processes on a stratified volcanic aquifer: Stable isotopes and dissolved gases in thermal waters of Vulcano Island (Aeolian archipelago). *Journal of Volcanology and Geothermal Research*, 192(3–4), 178–190. <https://doi.org/10.1016/j.jvolgeores.2010.02.020>
- Federico, C., Inguaggiato, S., Chacón, Z., Londoño, J. M., Gil, E., & Alzate, D. (2017). Vapour discharges on Nevado del Ruiz during the recent activity: Clues on the composition of the deep hydrothermal system and its effects on thermal springs. *Journal of Volcanology and Geothermal Research*, 346, 40–53. <https://doi.org/10.1016/j.jvolgeores.2017.04.007>
- Federico, C., Longo, M., D'Alessandro, W., Bellomo, S., Bonfanti, P., & Brusca, L. (2017). Hydrological versus volcanic processes affecting fluid circulation at Mt. Etna: Inferences from 10 years of observations at the volcanic aquifer. *Chemical Geology*, 452, 71–84. <https://doi.org/10.1016/j.chemgeo.2017.01.004>
- Finizola, A., Aubert, M., Revil, A., Schutze, C., & Sortino, F. (2009). Importance of structural history in the summit area of Stromboli during the 2002–2003 eruptive crisis inferred from temperature, soil CO₂, self-potential, and electrical resistivity tomography. *Journal of Volcanology and Geothermal Research*, 183(3–4), 213–227. <https://doi.org/10.1016/j.jvolgeores.2009.04.002>
- Finizola, A., Revil, A., Rizzo, E., Piscitelli, S., Ricci, T., Morin, J., et al. (2006). Hydrogeological insights at Stromboli volcano (Italy) from geoelectrical, temperature, and CO₂ soil degassing investigations. *Geophysical Research Letters*, 33(17), L17304. <https://doi.org/10.1029/2006GL026842>
- Finizola, A., Ricci, T., Deiana, R., Cabusson, S. B., Rossi, M., Praticelli, N., et al. (2010). Adventive hydrothermal circulation on Stromboli volcano (Aeolian Islands, Italy) revealed by geophysical and geochemical approaches: Implications for general fluid flow models on volcanoes. *Journal of Volcanology and Geothermal Research*, 196(1–2), 111–119. <https://doi.org/10.1016/j.jvolgeores.2010.07.022>
- Finizola, A., & Sortino, F. (2003). Preliminary model of fluid circulation at Stromboli volcano inferred by water and gas geochemistry. In *ICGG7-A-00108, 22–26 September 2003 Freiberg, Germany*.
- Finizola, A., Sortino, F., Lénat, J. F., Aubert, M., Ripepe, M., & Valenza, M. (2003). The summit hydrothermal system of Stromboli. New insights from self-potential, temperature, CO₂ and fumarolic fluid measurements, with structural and monitoring implications. *Bulletin of Volcanology*, 65(7), 486–504. <https://doi.org/10.1007/s00445-003-0276-z>
- Finizola, A., Sortino, F., Lénat, J.-F., & Valenza, M. (2002). Fluid circulation at Stromboli volcano (Aeolian Islands, Italy) from self-potential and CO₂ surveys. *Journal of Volcanology and Geothermal Research*, 116(1–2), 1–18. [https://doi.org/10.1016/s0377-0273\(01\)00327-4](https://doi.org/10.1016/s0377-0273(01)00327-4)
- Francalanci, L., Avanzinelli, R., Tommasini, S., & Heuman, A. (2007). West–east geochemical and isotopic traverse along the volcanism of the Aeolian Island arc, southern Tyrrhenian Sea, Italy: Inferences on mantle source processes. In L. Beccaluva, G. Bianchini, & M. Wilson (Eds.), *Cenozoic Volcanism in the Mediterranean Area* (pp. 235–263). Geological Society of America.

- Francalanci, L., Barbieri, M., Manetti, P., Peccerillo, A., & Tolomeo, L. (1988). Sr isotopic systematics in volcanic rocks from the island of Stromboli, Italy (Aeolian Arc). *Chemical Geology: Isotope Geoscience Section*, 73(2), 109–124. [https://doi.org/10.1016/0168-9622\(88\)90010-3](https://doi.org/10.1016/0168-9622(88)90010-3)
- Francalanci, L., Manetti, P., & Peccerillo, A. (1989). Volcanological and magmatological evolution of Stromboli volcano (Aeolian Islands): The roles of fractional crystallization, magma mixing, crustal contamination and source heterogeneity. *Bulletin of Volcanology*, 51(5), 355–378. <https://doi.org/10.1007/bf01056897>
- Francalanci, L., Manetti, P., Peccerillo, A., & Keller, J. (1993). Magmatological evolution of the Stromboli volcano (Aeolian Arc, Italy): Inferences from major and trace element and Sr-isotopic composition of lavas and pyroclastic rocks. *Acta Vulcanologica*, 3, 127–151.
- Francalanci, L., Tommasini, S., & Conticelli, S. (2004). The volcanic activity of Stromboli in the 1906–1998 period: Mineralogical, geochemical and isotope data relevant to the understanding of Strombolian activity. *Journal of Volcanology and Geothermal Research*, 131(1–2), 179–211. [https://doi.org/10.1016/s0377-0273\(03\)00362-7](https://doi.org/10.1016/s0377-0273(03)00362-7)
- Gasparini, C., Iannaccone, G., Scandone, P., & Scarpa, R. (1982). Seismotectonics of the Calabrian Arc. *Tectonophysics*, 84(2–4), 267–286. [https://doi.org/10.1016/0040-1951\(82\)90163-9](https://doi.org/10.1016/0040-1951(82)90163-9)
- Gat, J. R., & Carmi, I. (1970). Evolution of the isotopic composition of atmospheric waters in the Mediterranean Sea area. *Journal of Geophysical Research*, 75(15), 3039–3048. <https://doi.org/10.1029/JC075i015p03039>
- Gat, J. R., Shemesh, A., Tziperman, E., Hecht, A., Georgopoulos, D., & Basturk, O. (1996). The stable isotope composition of waters of the eastern Mediterranean Sea. *Journal of Geophysical Research: Oceans*, 101(C3), 6441–6451. <https://doi.org/10.1029/95jc02829>
- Gennaro, M. E., Grassa, F., Martelli, M., Renzulli, A., & Rizzo, A. L. (2017). Carbon isotope composition of CO₂-rich inclusions in cumulate-forming mantle minerals from Stromboli volcano (Italy). *Journal of Volcanology and Geothermal Research*, 346, 95–103. <https://doi.org/10.1016/j.jvolgeores.2017.04.001>
- Giggenbach, W. F. (1975). A simple method for the collection and analysis of volcanic gas samples. *Bulletin of Volcanology*, 39(1), 132–145. <https://doi.org/10.1007/bf02596953>
- Giudicepietro, F., Calvari, S., Alparone, S., Bianco, F., Bonaccorso, A., Bruno, V., et al. (2019). Integration of ground-based remote-sensing and in situ multidisciplinary monitoring data to analyze the eruptive activity of Stromboli volcano in 2017–2018. *Remote Sensing*, 11(15), 1813. <https://doi.org/10.3390/rs11151813>
- Grassa, F., Inguaggiato, S., & Liotta, M. (2008). Fluids geochemistry of Stromboli. In *The Stromboli Volcano: An integrated study of the 2002–2003 eruption*, AGU Geophysical Monograph (Vol. 182, pp. 49–63).
- Hilton, D. R., & Porcelli, D. (2013). Noble gases as mantle tracers. In H. D. Holland & K. K. Turekian (Eds.), *Treatise on Geochemistry* (2nd ed., pp. 293–325). Elsevier.
- Inguaggiato, C., Vita, F., Diliberto, I. S., & Calderone, L. (2017). The role of the aquifer in soil CO₂ degassing in volcanic peripheral areas: A case study of Stromboli Island (Italy). *Chemical Geology*, 469, 110–116. <https://doi.org/10.1016/j.chemgeo.2016.12.017>
- Inguaggiato, S., Diliberto, I. S., Federico, C., Paonita, A., & Vita, F. (2017). Review of the evolution of geochemical monitoring, networks and methodologies applied to the volcanoes of the Aeolian Arc (Italy). *Earth-Science Reviews*, 176, 241–276. <https://doi.org/10.1016/j.earscirev.2017.09.006>
- Inguaggiato, S., Diliberto, I. S., Federico, C., Paonita, A., & Vita, F. (2018). Review of the evolution of geochemical monitoring, networks and methodologies applied to the volcanoes of the Aeolian Arc (Italy). *Earth-Science Reviews*, 176, 241–276. <https://doi.org/10.1016/j.earscirev.2017.09.006>
- Inguaggiato, S., Hidalgo, S., Beate, B., & Bourquin, J. (2010). Geochemical and isotopic characterization of volcanic and geothermal fluids discharged from the Ecuadorian volcanic arc. *Geofluids*, 10(4), 525–541. <https://doi.org/10.1111/j.1468-8123.2010.00315.x>
- Inguaggiato, S., Jacome Paz, M. P., Mazot, A., Delgado Granados, H., Inguaggiato, C., & Vita, F. (2013). CO₂ output discharged from Stromboli Island (Italy). *Chemical Geology*, 339, 52–60. <https://doi.org/10.1016/j.chemgeo.2012.10.008>
- Inguaggiato, S., Martin-Del Pozzo, A. L., Aguayo, A., Capasso, G., & Favara, R. (2005). Isotopic, chemical and dissolved gas constraints on spring water from Popocatepetl (Mexico): Evidence of gas-water interaction magmatic component and shallow fluids. *Journal of Volcanology and Geothermal Research*, 141(1–2), 91–108. <https://doi.org/10.1016/j.jvolgeores.2004.09.006>
- Inguaggiato, S., Pecoraino, G., & D'Amore, F. (2000). Chemical and isotopic characterization of fluid manifestations of Ischia Island (Italy). *Journal of Volcanology and Geothermal Research*, 99(1–4), 151–178. [https://doi.org/10.1016/s0377-0273\(00\)00158-x](https://doi.org/10.1016/s0377-0273(00)00158-x)
- Inguaggiato, S., & Rizzo, A. (2004). Dissolved helium isotope ratios in ground-waters: A new technique based on gas-water re-equilibration and its application to Stromboli volcanic system. *Applied Geochemistry*, 19(5), 665–673. <https://doi.org/10.1016/j.apgeochem.2003.10.009>
- Inguaggiato, S., Vita, F., Cangemi, M., & Calderone, L. (2019). Increasing summit degassing at the Stromboli volcano and relationships with volcanic activity (2016–2018). *Geosciences*, 9(4), 176. <https://doi.org/10.3390/geosciences9040176>
- Inguaggiato, S., Vita, F., Cangemi, M., & Calderone, L. (2020). Changes in CO₂ soil degassing style as a possible precursor to volcanic activity: The 2019 case of Stromboli paroxysmal eruptions. *Applied Sciences*, 10(14), 4757. <https://doi.org/10.3390/app10144757>
- Inguaggiato, S., Vita, F., Cangemi, M., Inguaggiato, C., & Calderone, L. (2021). The monitoring of CO₂ soil degassing as Indicator of Increasing volcanic activity: The paroxysmal activity at Stromboli Volcano in 2019–2021. *Geosciences*, 11(4), 169. <https://doi.org/10.3390/geosciences11040169>
- Inguaggiato, S., Vita, F., Cangemi, M., Mazot, A., Sollami, A., Calderone, L., et al. (2017). Stromboli volcanic activity variations inferred from observations of fluid geochemistry: 16 years of continuous monitoring of soil CO₂ fluxes (2000–2015). *Chemical Geology*, 469, 69–84. <https://doi.org/10.1016/j.chemgeo.2017.01.030>
- Inguaggiato, S., Vita, F., Rouwet, D., Bobrowski, N., Morici, S., & Sollami, A. (2011). Geochemical evidence of the renewal of volcanic activity inferred from CO₂ soil and SO₂ plume fluxes: The 2007 Stromboli eruption (Italy). *Bulletin of Volcanology*, 73(4), 443–456. <https://doi.org/10.1007/s00445-010-0442-z>
- Lages, J., Rizzo, A. L., Aiuppa, A., Robidoux, P., Aguilar, R., Apaza, F., & Masias, P. (2021). Crustal controls on light noble gas isotope variability along the Andean Volcanic Arc. *Geochemical Perspectives Letters*, 19, 45–49. <https://doi.org/10.7185/geochemlet.2134>
- Landi, P., Corsaro, R. A., Francalanci, L., Civetta, L., Miraglia, L., Pompilio, M., & Tesoro, R. (2009). Magma dynamics during the 2007 Stromboli eruption (Aeolian Islands, Italy). Mineralogy, geochemistry and isotope data. *Journal of Volcanology and Geothermal Research*, 182(3–4), 255–268. <https://doi.org/10.1016/j.jvolgeores.2008.11.010>
- Lénat, J. F., Bachélery, P., & Peltier, A. (2012). The interplay between collapse structures, hydrothermal systems, and magma intrusions: The case of the central area of Piton de la Fournaise volcano. *Bulletin of Volcanology*, 74(2), 407–421. <https://doi.org/10.1007/s00445-011-0535-3>
- Liotta, M., Brusca, L., Grassa, F., Inguaggiato, S., Longo, M., & Madonia, P. (2006). Geochemistry of rainfall at Stromboli volcano (Aeolian Islands): Isotopic composition and plume-rain interaction. *Geochemistry, Geophysics, Geosystems*, 7, Q07006. <https://doi.org/10.1029/2006GC001288>
- Liotta, M., & Martelli, M. (2012). Dissolved gases in brackish thermal waters: An improved analytical method. *Geofluids*, 12(3), 236–244. <https://doi.org/10.1111/j.1468-8123.2012.00365.x>
- Lorenz, V., & Kurszlaukis, S. (2007). Root zone processes in the phreatomagmatic pipe emplacement model and consequences for the evolution of maar-diatreme volcanoes. *Journal of Volcanology and Geothermal Research*, 159(1–3), 4–32. <https://doi.org/10.1016/j.jvolgeores.2006.06.019>

- Lupton, J., Lilley, M., Butterfield, D., Evans, L., Embley, R., Massoth, G., et al. (2008). Venting of a separate CO₂-rich gas phase from submarine arc volcanoes: Examples from the Mariana and Tonga-Kermadec arcs. *Journal of Geophysical Research*, *113*(B8), B08S12. <https://doi.org/10.1029/2007JB005467>
- Madonia, P., Campilongo, G., Cangemi, M., Carapezza, M. L., Inguaggiato, S., Ranaldi, M., & Vita, F. (2021). Hydrogeological and geochemical characteristics of the coastal aquifer of Stromboli Volcanic Island (Italy). *Water*, *13*(4), 417. <https://doi.org/10.3390/w13040417>
- Martelli, M., Rizzo, A. L., Renzulli, A., Ridolfi, F., Arienzo, I., & Rosciglione, A. (2014). Noble-gas signature of magmas from a heterogeneous mantle wedge: The case of Stromboli volcano (Aeolian Islands, Italy). *Chemical Geology*, *368*, 39–53. <https://doi.org/10.1016/j.chemgeo.2014.01.003>
- Mauri, G., Saracco, G., Labazuy, P., & Williams-Jones, G. (2018). Correlating hydrothermal system dynamics and eruptive activity – A case-study of Piton de la Fournaise volcano, La Réunion. *Journal of Volcanology and Geothermal Research*, *363*, 23–39. <https://doi.org/10.1016/j.jvolgeores.2018.08.009>
- Métrich, N., Bertagnini, A., & Di Muro, A. (2010). Conditions of magma storage, degassing and ascent at Stromboli: New insights into the volcano plumbing system with inferences on the eruptive dynamics. *Journal of Petrology*, *51*(3), 603–626. <https://doi.org/10.1093/petrology/egp083>
- Métrich, N., Bertagnini, A., & Pistolesi, M. (2021). Paroxysms at Stromboli Volcano (Italy): Source, genesis and dynamics. *Frontiers in Earth Science*, *9*, 593339. <https://doi.org/10.3389/feart.2021.593339>
- Morelli, C., Giese, P., Cassinis, R., Colombi, B., Guerra, I., Luongo, G., et al. (1975). Crustal structure of Southern Italy. A seismic refraction profile between Puglia–Calabria–Sicily. *Bollettino di Geofisica Teorica ed Applicata*, *18*, 183–210.
- Ohsawa, S., Kazahaya, K., Yasuhara, M., Kono, T., Kitaoka, K., Yusa, Y., & Yamaguchi, K. (2002). Escape of volcanic gas into shallow groundwater systems at Unzen volcano (Japan): Evidence from chemical and stable carbon isotope compositions of dissolved inorganic carbon. *Limnology*, *3*(3), 0169–0173. <https://doi.org/10.1007/s102010200020>
- Osinski, G. R., Spray, J. G., & Lee, P. (2001). Impact-induced hydrothermal activity within the Houghton impact structure, arctic Canada: Generation of a transient, warm, wet oasis. *Meteoritics & Planetary Science*, *36*(5), 731–745. <https://doi.org/10.1111/j.1945-5100.2001.tb01910.x>
- Panza, G. F., Peccerillo, A., Aoudia, A., & Farina, B. (2007). Geophysical and petrological modelling of the structure and composition of the crust and upper mantle in complex geodynamic settings: The Tyrrhenian Sea and surroundings. *Earth-Science Reviews*, *80*(1–2), 1–46. <https://doi.org/10.1016/j.earscirev.2006.08.004>
- Paonita, A., Longo, M., Bellomo, S., D'Alessandro, W., & Brusca, L. (2016). Dissolved inert gases (He, Ne and N₂) as markers of groundwater flow and degassing areas at Mt Etna volcano (Italy). *Chemical Geology*, *443*, 10–21. <https://doi.org/10.1016/j.chemgeo.2016.09.018>
- Prano, V., & Liotta, M. (2018). Precisione e accuratezza nella determinazione dei costituenti maggiori in soluzione acquosa mediante cromatografia ionica: Stime per i cromatografi Dionex ICS-1100 utilizzati presso la Sezione INGV di Palermo, *INGV Technical Reports*. <https://doi.org/10.13127/rpt/390>
- Revil, A., Finizola, A., Ricci, T., Delcher, E., Peltier, A., Barde-Cabusson, S., et al. (2011). Hydrogeology of Stromboli volcano, Aeolian Islands (Italy) from the interpretation of resistivity tomograms, self-potential, soil temperature and soil CO₂ concentration measurements. *Geophysical Journal International*, *186*(3), 1078–1094. <https://doi.org/10.1111/j.1365-246x.2011.05112.x>
- Revil, A., & Linde, N. (2006). Chemico-electromechanical coupling in microporous media. *Journal of Colloid and Interface Science*, *302*(2), 682–694. <https://doi.org/10.1016/j.jcis.2006.06.051>
- Rizzo, A., Aiuppa, A., Capasso, G., Grassa, F., Inguaggiato, S., Longo, M., & Carapezza, M. L. (2008). The 5 April 2003 paroxysm at Stromboli: A review of geochemical observations. In *Learning from Stromboli and its 2002–2003 eruptive crisis*, American Geophysical Union *Geophysical Monograph Series* (Vol. 182, pp. 347–358). American Geophysical Union.
- Rizzo, A., Grassa, F., Inguaggiato, S., Liotta, M., Longo, M., Madonia, P., et al. (2009). Geochemical evaluation of observed changes in volcanic activity during the 2007 eruption at Stromboli (Italy). *Journal of Volcanology and Geothermal Research*, *182*(3–4), 246–254. <https://doi.org/10.1016/j.jvolgeores.2008.08.004>
- Rizzo, A. L., Caracausi, A., Chavagnac, V., Nomikou, P., Polymenakou, P., Mandalakis, M., et al. (2016). Kolombo submarine volcano (Greece): An active window into the Aegean subduction system. *Scientific Reports*, *6*(1), 28013. <https://doi.org/10.1038/srep28013>
- Rizzo, A. L., Caracausi, A., Chavagnac, V., Nomikou, P., Polymenakou, P. N., Mandalakis, M., et al. (2019). Geochemistry of CO₂-rich gases venting from submarine volcanism: The case of Kolombo (Hellenic Volcanic Arc, Greece). *Frontiers in Earth Science*, *7*, 60. <https://doi.org/10.3389/feart.2019.00060>
- Rizzo, A. L., Federico, C., Inguaggiato, S., Sollami, A., Tantillo, M., Vita, F., et al. (2015). The 2014 effusive eruption at Stromboli volcano (Italy): Inferences from soil CO₂ flux and ³He/⁴He ratio in thermal waters. *Geophysical Research Letters*, *42*(7), 2235–2243. <https://doi.org/10.1002/2014GL062955>
- Rizzo, A. L., Robidoux, P., Aiuppa, A., & Di Piazza, A. (2022). ³He/⁴He signature of magmatic fluids from Telica (Nicaragua) and Baru (Panama) volcanoes, Central American Volcanic Arc. *Applied Sciences*, *12*(9), 4241. <https://doi.org/10.3390/app12094241>
- Robidoux, P., Rizzo, A., Aguilera, F., Aiuppa, A., Artale, M., Liuzzo, M., et al. (2020). Petrological and noble gas features of Lascar and Lastarria volcanoes (Chile): Inferences on plumbing systems and mantle characteristics. *Lithos*, *370–371*, 105615. <https://doi.org/10.1016/j.lithos.2020.105615>
- Rosi, M., Bertagnini, A., & Landi, P. (2000). Onset of the persistent activity at Stromboli volcano (Italy). *Bulletin of Volcanology*, *62*(4–5), 294–300. <https://doi.org/10.1007/s004450000098>
- Sander, R. (2015). Compilation of Henry's law constants (version 4.0) for water as solvent. *Atmospheric Chemistry and Physics*, *15*(8), 4399–4981. <https://doi.org/10.5194/acp-15-4399-2015>
- Schiavi, F., Kobayashi, K., Nakamura, E., Tiepolo, M., & Vannucci, R. (2012). Trace element and Pb–B–Li isotope systematics of olivine-hosted melt inclusions: Insights into source metasomatism beneath Stromboli (southern Italy). *Contributions to Mineralogy and Petrology*, *163*(6), 1011–1031. <https://doi.org/10.1007/s00410-011-0713-5>
- Simmons, S. F., & Christenson, B. W. (1994). Origins of calcite in a boiling geothermal system. *American Journal of Science*, *294*(3), 361–400. <https://doi.org/10.2475/ajs.294.3.361>
- Singaraja, C., Chidambaram, S., & Jacob, N. (2018). A study on the influence of tides on the water table conditions of the shallow coastal aquifers. *Applied Water Science*, *8*(1), 11. <https://doi.org/10.1007/s13201-018-0654-5>
- Taran, Y., Kalacheva, E., Inguaggiato, S., Cardellini, C., & Karpov, G. (2017). Hydrothermal systems of the Karymsky Volcanic Centre, Kamchatka: Geochemistry, time evolution and solute fluxes. *Journal of Volcanology and Geothermal Research*, *346*, 28–39. <https://doi.org/10.1016/j.jvolgeores.2017.05.023>
- Tommasini, S., Heumann, A., Avanzinelli, R., & Francalanci, L. (2007). The fate of high-angle dipping slabs in the subduction factory: An integrated trace element and radiogenic isotope (U, Th, Sr, Nd, Pb) study of Stromboli volcano, Aeolian Arc, Italy. *Journal of Petrology*, *48*(12), 2407–2430. <https://doi.org/10.1093/petrology/egm066>

- Vita, F., Inguaggiato, S., Capasso, G., Liotta, M., & Rizzo, A. L. (2023). Chemical-physical parameters, major, and minor elements composition of thermal waters from 8 wells in the Stromboli aquifer (Italy), Version 1.0 [Dataset]. Interdisciplinary Earth Data Alliance (IEDA). <https://doi.org/10.26022/IEDA/112932>
- Webster, J. D., & Mandeville, C. W. (2007). Fluid immiscibility in volcanic environments. *Reviews in Mineralogy and Geochemistry*, 65(1), 313–362. <https://doi.org/10.2138/rmg.2007.65.10>
- Weinstein, Y. (2007). A transition from strombolian to phreatomagmatic activity induced by a lava flow damming water in a valley. *Journal of Volcanology and Geothermal Research*, 159(1–3), 267–284. <https://doi.org/10.1016/j.jvolgeores.2006.06.015>
- Yamada, M., Ohsawa, S., Kazahaya, K., Yasuhara, M., Takahashi, H., Amita, K., et al. (2011). Mixing of magmatic CO₂ into volcano groundwater flow at Aso volcano assessed combining carbon and water stable isotopes. *Journal of Geochemical Exploration*, 108(1), 81–87. <https://doi.org/10.1016/j.gexplo.2010.10.007>